DEVELOPMENT OF RELATIONSHIPS AND TRENDING METHODOLOGIES FOR RAILROAD TRACK COMPONENT AND GEOMETRY DATA

BY

ARTHUR MORGADO BILHERI T CARVALHO

THESIS

Submitted in partial fulfillment of the requirements
for the degree of Master of Science in Civil Engineering
in the Graduate College of the
University of Illinois Urbana-Champaign, 2023

Urbana, Illinois

Adviser:

Assistant Professor J. Riley Edwards

ABSTRACT

The safe and efficient movement of trains requires periodic inspection of the geometry of the track system and health of its components. Railroads have used laser-based track geometry testing to comply with regulatory requirements and internal business practices for over 30 years. More recently, these systems have been supplemented by new technologies capable of inspecting many other attributes of the track including subgrade condition, track component health, and ballast profile. Computational advances including machine vision and artificial intelligence, and the application of big data, have drastically increased the value that can be derived from the ever-growing track health dataset. In this thesis, I present a method to manage the flow of data in a railroad, starting from field data collection to multi-year capital plans. In my case study, geometry and track component data were collected over a 115-mile (185 km) heavy haul Class I railroad subdivision in the US and were analyzed for correlations. One of the primary challenges to using track-related data collected from multiple inspection systems on different days is aligning datasets. In this research, datasets are aligned using fixed assets (switches and crossings). After aligning the datasets, fixed windows and aggregation functions are used to analyze the data. Correlation matrices and scatter plots of static data from both technologies showed little correlation between the two datasets. This suggests that railroads should consider the use of both technologies to comply with federal regulations, monitor the condition of their components and infrastructure, and ensure the safe movement of trains. Additionally, a trending framework is developed that is suitable for both geometry and component data, providing useful information to develop comprehensive maintenance plans to facilitate reliable and efficient passenger and freight movement.

ACKNOWLEDGMENTS

I am sure that I will lack in English vocabulary to acknowledge all the people that have contributed to this immense endeavor of moving abroad, living in a different language and culture, while reconciling classes, research, and work. First, I would like to thank my mother and grandmother for being the family God chose for me. Also, my friends in Brazil and at Urbana-Champaign who made these two years a lot easier to come through. Special thanks are due to the B118 folks for participating and engaging in the social events we organized together and making the basement a more fun place to spend days.

To the RailTEC team, Riley Edwards, Marcus Dersch, and Arthur Lima, thanks for giving me the opportunity to study and work with this amazing group. To Chris Barkan, Tyler Dick, and Conrad Ruppert, thank you for sharing with me the passion about railroads and trains and also for engaging in model trains, happy hour, and other railfanning-related events which contributed a lot to the learning process.

This project would never come to fruition without the industry partners: Brad Spencer (CSX), Aarron Brown (UP), David Wenrich (FEC), Richard Fox-Ivey, and Antonio Mauricio (Railmetrics). Thank you for supporting this research project.

There are truly no words to express my gratitude to the MRS Logistica team that supported and encouraged me to seek a master's degree while still working on awesome projects remotely. Special thanks to Danilo Vieira and Anelise Salzani for not measuring efforts in making all the arrangements necessary for having an employee working abroad and Josue Bastos for putting me in contact with the RailTEC team.

I would like to express sincere appreciation to the Federal Railroad Administration (FRA) in general and Cam Stuart specifically for providing support for this project, including funding, insights, and industry connections, without which this research would not be possible.

To my family:

Minhas raízes estão no ar

Minha casa é qualquer lugar

Voando sem instrumentos

Ao sabor do vento

Toda vida, o dia inteiro

Não seria exagero

Se depender de mim, eu vou até o fim

Cada célula, todo fio de cabelo

Falando assim parece exagero

Mas se depender de mim, eu vou até o fim

Até o fim

Engenheiros do Hawaii

TABLE OF CONTENTS

CHAPTER 1: INTRODUCTION

1.1 Track Geometry Inspection and Regulatory Requirements

The desired maximum operating speed for a segment of railway track dictates the required geometric tolerances and track quality that must be maintained. These, in turn, relate to the frequency and magnitude of permissible wheel loads, desired level of service, risk, and network resiliency. To benefit from the economies of scale that are inherent to rail transportation, axle loads must be maximized. Axle load increases, while economically justified, have adverse impacts on the track structure and its components, and the geometry of the track system.

Track classes refer to different categories or classifications of track based on their maximum allowable speed for freight and passenger trains. These classifications help the railroads manage their infrastructure objectively and ensure the safe and efficient operation of trains. In the United States (US), track classes are defined in the US Department of Transportation (DOT) Federal Railroad Administration (FRA) Track Safety Standards (CFR 213) (FRA, 2022). Table 1.1 provides a summary of the most common FRA track classes and maximum allowable train operating speeds.

Table 1.1: FRA Track classes and allowable train speeds

FRA Track Class	Maximum Allowable Train Speed [mph (km/h)]	
	Freight Trains	Passenger Trains
0 (Excepted)	10 (16)	Not Allowed
1	10 (16)	15 (24)
2	25 (40)	30 (48)
3	40 (64)	60 (97)
4	60 (97)	80 (129)
5	80 (129)	90 (145)

Track quality is most commonly quantified through its geometry parameters (Esveld, 2001). To comply with FRA regulatory thresholds, avoid exceptions and fines, and to ensure the safe movement of trains, railroads conduct periodic geometry inspections. FRA (2022) requires railroads to conduct inspections between one and four times per year depending on FRA track class and annual traffic measured in million gross tons (MGT) (Table 1.2).

Table 1.2: FRA-mandated minimum number of inspections per year

	Annual Tonnage (MGT)				
	Freight Trains			Passenger Trains	
Track Class	< 40	40 - 60	> 60	< 20	>= 20
0 (Excepted)	0	0	0	n/a	n/a
1	0	0	0	0	0
2	0	0	0	1	1
3	1	2	2	2	2
4	2	3	4	2	3
5 and above	2	3	4	3	3

For each track class, FRA defines the track geometry tolerances that must be maintained (Table 1.3). If any of the thresholds are exceeded, temporary speed restrictions (i.e. slow orders) must be put in place and maintenance conducted to restore geometry to that of the original track class. Temporary speed restrictions increase operating costs, reduce network velocity, and increase transit times for goods and people. To avoid speed restrictions and optimize maintenance spending, railroads use forecasting to predict when and where geometry thresholds are met and exceeded (Esveld, 2014).

Table 1.3: FRA-mandated track geometry thresholds for each track class

Track Geometry Condition	Geometry thresholds [inch (mm)]					
	0 (Excepted)	**1**	**2**	**3**	**4**	**5**
Tight Gauge negative deviation from nominal gauge: 4' 8. 5", 56. 5 in, 1435mm	n/a	0.5 (13)	0.5 (13)	0.5 (13)	0. 5 (13)	0. 5 (13)
Wide Gauge positive deviation from nominal gauge: 4' 8. 5", 56. 5 in, 1435 mm	1.8 (45)	1.5 (38)	1.3 (33)	1.3 (33)	1.0 (25)	1.0 (25)
Track Alignment 62' - Tangent Deviation from the mid-offset from a 62' (20m) chord	n/a	5 (127)	3 (76)	1.75 (44)	1.5 (38)	0.75 (19)
Track Alignment 62' - Curve Deviation from the mid-offset from a 62' (20m) chord	n/a	5 (127)	3 (76)	1.75 (44)	1.5 (38)	0.625 (16)
Track Alignment 31' - Tangent Deviation from the mid-offset from a 31' (10m) chord	n/a	n/a	n/a	1.25 (32)	1.0 (25)	0.5 (13)
Runoff Runoff in any 31' (10m) of rail at the end of a raise	n/a	3.5 (89)	3 (76)	2 (51)	1.5 (38)	1.0 (25)
Profile 62' The deviation from uniform profile at the mid-ordinate of a 62' (20m) chord	n/a	3 (76)	2 (51)	2.25 (57)	2 (51)	1.25 (32)
Profile 31' The deviation from uniform profile at the mid-ordinate of a 31' (10m) chord	n/a	n/a	n/a	1.0 (25)	1.0 (25)	1.0 (25)
Warp 62' Difference in crosslevel between any two points less than 62' (20m) apart	n/a	3 (76)	2.25 (57)	2 (51)	1.75 (44)	1.5 (38)
Warp 10' Difference in crosslevel between any two points less than 10' (3m) apart	n/a	2.25 (57)	2.25 (57)	1.75 (44)	1.25 (32)	1.0 (25)
Twist 31' The difference on crosslevel in spirals between two points 31' (20m) apart	n/a	2 (51)	1.75 (44)	1.25 (32)	1.0 (25)	0.75 (19)

In addition to the aforementioned requirements for periodic track geometry inspections, the FRA requires railroads to conduct manual visual inspections. These inspections are usually carried out by a designated (and qualified) railroad employee that is commonly referred to as a *Track Inspector* who travels over a length of track in a hi-rail vehicle. A hi-rail vehicle can operate on both highways and railroad track and allow access to the track at highway-rail grade crossings of sufficient length. The frequency of this type of inspection is also defined by the FRA (2022) (Table 1.4) with most of the primary rail corridors in the US (FRA Classes 4 and 5) requiring visual inspections twice per week.

Table 1.4: FRA requirements for visual track inspection frequency

FRA Track Class	Track Type	Required Frequency
0 (Excepted), 1, 2, 3	Main track and sidings	Weekly with at least 3 calendar days interval between inspections, or before use, if the track is used less than once a week, or twice weekly with at least 1 calendar day interval between inspections, if the track carries passenger trains or more than 10 million gross tons of traffic during the preceding calendar year.
0 (Excepted), 1, 2, 3	Other than main track and sidings	Monthly with at least 20 calendar days interval between inspections.
4 and 5	All tracks	Twice weekly with at least 1 calendar day interval between inspections

The FRA requires that this type of inspection be undertaken at slow speed due to its visual nature. Some inspections are carried out at speeds of 30 mph (48 km/h) or less, and almost all inspections are carried out at speeds that are lower than the maximum train operating speed. This has an impact on train flow and operations and can present a challenge for accessing infrastructure given many of the primary rail corridors in the US are operating at or near

capacity. Additionally, FRA rules do not allow this class of railroad employee to work more than 10 hours a day, thereby limiting the amount of track that can be inspected on a given day when considering track occupancy challenges. The length of track that can reasonably be inspected in a single shift is around 100 miles (160 km).

It is neither prudent nor economical to repair the same defects at a given location in a recurring and reactive manner. Thus, developing and applying a framework for track geometry data trending is an essential step toward achieving a strategy for predictive maintenance. Predictive maintenance requires a large amount of data, which are used to create models that can predict when maintenance should be conducted to restore track quality. Predictive maintenance models increase network reliability, reduce track infrastructure down time, and minimize the required use of slow orders (Neuhold et al., 2020).

The trending framework I will present relies on a comprehensive, yet simple, model. In some ways this model compromises accuracy due to its comprehensive nature when compared to a more sophisticated model with higher accuracy (albeit less comprehensive). A simple model helps to disseminate information among many levels in the rail management hierarchy given the outputs are easier to understand and act upon (Jovanovic, 2004). Having a more sophisticated model tends to produce information that is only relevant to certain levels of the company, limiting its acceptance and use throughout the organization and network (Liao et al., 2022).

A case study is presented in Chapters 2 and 3 using geometry data collected from Autonomous Track Geometry Measurement Systems (ATGMS) from a Class I railroad in the US. Additionally, track component inspection data were collected using the Laser Rail Inspection System (LR*AI*L) developed by Railmetrics Inc. (Harrington et al., 2022) for a period of approximately one year that overlaps with ATGMS data collection. Both types of data were

collected on a 115-mile (185 km) section of a high-density (90 MGT annually) single-track rail corridor in the southeastern US.

1.2 Railway Track Inspection Data

To ensure the safe movement of trains, railroads routinely assess the condition of their track components including rails, crossties, and fastening systems. This is most commonly conducted through human visual inspections as mandated by FRA (2022) and introduced in Section 1.1. In addition to these visual assessments, the system-level condition of tracks is measured using its geometry parameters (Table 1.3).

1.2.1 Geometry

Geometry refers broadly to the geometric position and condition of railroads curves and tangents, related to their design, use, and maintenance (Hay, 1982). Track geometry most commonly describes the position of the rails in horizontal, longitudinal, and vertical planes. It includes design features (e.g. tangent, transition curves, curves, superelevation) as well as irregularities in which the track's position deviates from the original design geometry (Keylin, 2019). These irregularities cause the track to deteriorate faster due to higher dynamic forces (Esveld, 2014). When these irregularities exceed certain thresholds maintained and regulated by the FRA (2022), they are referred to as geometry defects or exceptions.

1.2.2 Geometry Inspection Vehicles

Geometry inspection is conducted using a specialized vehicle, commonly referred to as a *geometry inspection car* or *geometry recording car*. Geometry cars can be a rail-bound vehicle, either self-propelled or towed, or a hi-rail vehicle (Carr et al., 2009).

Inspection vehicles can be either manned (when an operator rides inside the vehicle during inspection) or unmanned (when the system collects data autonomously without the need for an operator) (Figure 1.1). The unmanned classification refers only to the geometry measurement system that is capable of operating autonomously, not to the operation of the car itself. Hi-rail vehicles can only be unmanned if they are already on the railroad tracks (rail bound). The following sub-sections discuss the advantages and disadvantages of each classification of geometry inspection system.

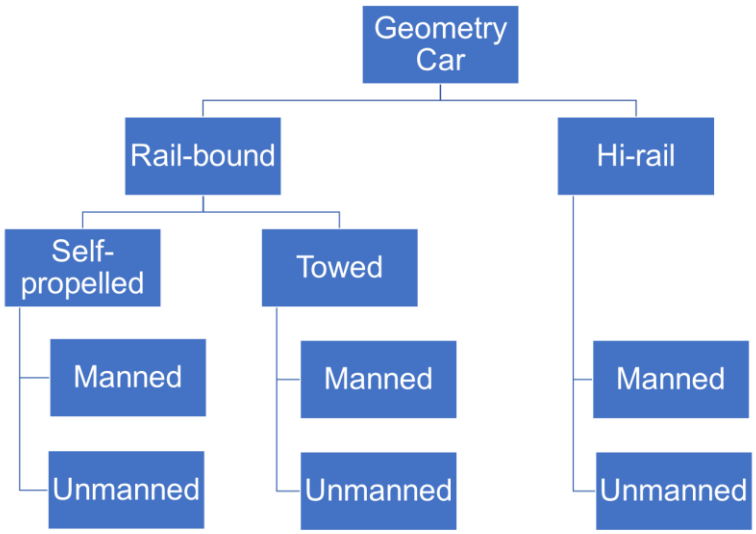

Figure 1.1: Common platforms for track geometry inspection cars

1.2.2.1 Rail-bound Self-propelled Manned Vehicles

Initial versions of geometry testing vehicles were rail-bound, manned cars equipped with facilities for railway personnel, generators, prime movers, and inspection equipment (Figure 1.2).

Due to their high utilization and need to travel over large networks for extended periods of time, these cars featured small kitchens and crew bedrooms. Depending on FRA regulations and individual railroad operating practices, engineering staff could operate the car without a transportation crew or locomotive. Their specialized design included independent power generation and allowed integration of additional inspection systems for rail and catenary.

Figure 1.2: Rail-bound self-propelled manned vehicle (photo credit: CSX)

Although some self-propelled vehicles can travel at typical mainline train speeds – or even at high speed, such as the geometry cars used in high-speed lines in Japan and Germany – this is not true for the majority of rail bound inspection cars. This results in conflicts with revenue service train operations and also presents challenges with changing crews and storing the equipment in yards or storage tracks during overnight periods when testing is not typically conducted.

1.2.2.2 Rail-bound Manned Towed Vehicles

Rail-bound manned towed vehicles are often repurposed passenger railcars (Figure 1.3) that are adapted to include measurement systems, power generation, and room for operating personnel. They combine the benefits of self-propelled cars while retaining the structural elements and special design features (such as trucks and draft gears) found in passenger cars built for higher speed revenue service, thereby allowing these cars to travel up to the maximum allowable speed for passenger trains. If a dedicated locomotive is assigned to this train, it can provide power to the railcars. However, a drawback to this approach is that the locomotive must be equipped with all the train control systems used by the railroad and adhere to various operating requirements, including axle-load and axle count specifications.

Figure 1.3: Example manned rail-bound geometry vehicle towed by a locomotive (photo credit: CSX)

1.2.2.3 Hi-rail Manned Vehicles

Hi-rail vehicles (Figure 1.4) are primarily employed for maintenance of way (MOW) tasks and visual inspections. They offer flexibility in accessing the tracks at highway-rail grade crossings. This reduces their impact on revenue trains caused by their reduced speed, which is typically limited to 45 mph (72 km/h). Additionally, they do not require a dedicated storage

track, as they can be parked overnight at the railroad's office or any other surface parking location. Another element of their flexibility lies in their short stopping distance, enabling operators to easily stop the vehicle for defect verification or manual measurements.

Figure 1.4: Example image of a hi-rail geometry vehicle

1.2.2.4 Rail-bound Unmanned Towed Vehicles

The most common form of rail-bound unmanned towed geometry inspection vehicle is the ATGMS. Benefits of ATGMS stem primarily from their cost-effectiveness (Carr et al., 2009). Operating without a crew allows these systems to function around the clock, covering distances in excess of 500 miles in a single day, far surpassing what is possible with a manned vehicle. Such high utilization enables railroads to reduce inspection intervals on the busiest corridors from four times a year to as frequent as three times a week. This increased frequency of inspections results in a substantial rise in the volume of collected data, necessitating the implementation of a robust asset management platform capable of handling large datasets.

When there is a crew onboard the geometry car, the operator is tasked with detecting outliers and monitoring the equipment's health to identify erroneous data, such as measurement errors, which can lead to improper detection of exceptions. In the absence of onboard personnel, defect validation must be performed using filters during the inspection process or manually validated after the inspection is conducted.

Unmanned inspection vehicles rely on Global Positioning Systems (GPS) and encoders for location identification rather than the input from the operator. This method, while generally reliable, is known to induce errors related to incorrect track labeling or milepost location, and these must be addressed in the office. Some railroads use Differential GPS (DGPS) or Radio Frequency Identification (RFID) tags to increase location accuracy. This is especially important for rail transit systems that operate in tunnels where GPS signals are non-existent. Relying only on GPS also requires the railroad to provide an accurate and reliable Geographic Information System (GIS) database for the system for use in locating the measurements. If a low precision GIS database is provided location determination (e.g. milepost and track) will be affected, resulting in errors such as misidentified track (e.g. Track 1 vs. Track 2) (Bilheri et al., 2023).

The most common platform for ATGMS deployment is revenue vehicles, such as locomotives (Figure 1.5), boxcars (Figure 1.6), or passenger coaches (Figure 1.7). Such vehicles offer the advantage of being used within the regular revenue service operational cycle, avoiding conflicts associated with track occupancy solely for the purpose of track inspection. However, in the case of specially designed boxcars, the power supply must come from rooftop solar panels or an onboard generator. In contrast, locomotives or passenger coaches already have the necessary power supply. The system should be small enough to fit in the vehicle, without interfering with

other systems and have low maintenance requirements, including calibration, that should match the normal schedule of the host vehicle to avoid additional stops (Scott et al., 2010).

Figure 1.5: Example of locomotive mounted ATGMS used in Brazil

Figure 1.6: Example of boxcar mounted ATGMS used in the US

Figure 1.7: Example of passenger car mounted ATGMS in the US (photo credit: ENSCO)

Certain railroads have opted to repurpose locomotives for ATGMS operations (Figure 1.8) by removing their prime mover, traction motors, control stands, and other devices and installing generators, air conditioning systems, and necessary measurement components (Railway Track and Structures, 2020). This approach offers the advantage of utilizing a six-axle truck, which enhances lateral forces and tests the track under a more realistic loading environment without the need to invest in new assets. These repurposed locomotives can operate on a special train or within a revenue service consist, functioning as a car without providing tractive effort.

Other railroads have chosen to upgrade their manned geometry cars to operate autonomously, transforming them into crewless special trains. While highly efficient for inspections, these systems still require their own operational windows and conflict with revenue trains (BNSF, 2021).

Figure 1.8: Example image of repurposed locomotive used for ATGMS operations

1.2.2.5 Hi-rail Unmanned Vehicles

This platform comprises a hi-rail trailer equipped with measurement systems capable of autonomous operation, being towed by another vehicle, or operating in a remote control scenario (RailPod, 2021).

1.2.2.6 Sampling Frequency

FRA (2022) regulations require geometry measurement systems to maintain a distance-based sampling interval not exceeding five feet (1.52 m). Presently, all commercial track geometry systems operate with a higher frequency, commonly capturing one measurement per

foot (0.30 m) or every 25 cm (0.8 ft) if the system operates in metric units. This results in 5,280 samples per mile or 4,000 samples per kilometer.

1.2.2.7 Measurement Channels

Geometry measurement types, which are individually referred to as channels, must include the FRA-mandated calculations as specified in Table 1.5. However, most systems are capable of measuring many additional channels (FRA, 2022) (Table 1.5). Additional channels and data can be used for studying correlations with other inspection tools (Goodarzi et al., 2020), running Multi-body Dynamic Simulation (MBS) tools (Keylin, 2019), or to generate Track Quality Indexes (TQI) to assess the condition and degradation of track (Neuhold et al., 2020).

Table 1.5: Geometry measurement channels and descriptions (FRA 2022)

Measurement	Required by FRA?	Description
Gauge	Yes	Distance between the two rail gauge faces, measured 5/8” below the top of the rail.
Base Gauge	No	Distance between the closest points of the rail bases.
Curvature	Indirectly	Track curvature: used to identify tangent, spirals and curve body.
Cross level	Yes	Measured difference in height between both rails.
Twist 31’	Yes	Difference in cross level between two points 31’ apart. Also known as Long Twist.
Twist 22’	No	Difference in cross level between two points 21’ apart. Also known as Medium Twist.
Twist 11’	Yes	Difference in cross level between two points 11’ apart. Also known as Short Twist.
Warp	Yes	Difference in crossover between any two points less than 62’ apart.
Alignment	Yes	Deviation from uniform alignment of the left and right rail measured on the center of a 31’, 62’, and 124’ chord lengths (only for FRA Class 6 and above).
Profile	Yes	Deviation from uniform Profile of the left and right rail measured on the center of a 31’, 62’ and 124’ chord lengths (only for FRA Class 6 and above).
Alignment Space Curve	No	Absolute alignment deviation of the left and right rail from design.
Profile Space Curve	No	Absolute profile deviation of the left and right rail from design.
Gradient	No	Longitudinal gradient of the track.
Rail Cant	Yes, for concrete crossties	The rotation of the left and right rail along the longitudinal axis.
Speed	No	Recorded speed of the measuring vehicle.

In addition to the above measurements, other descriptive information is collected on a foot-by-foot basis including GPS coordinates, milepost, inspection date, track inspected, railroad division and subdivision names, posted FRA track class, and current operating speed. These additional forms of data help with subsequent data organization and storage.

1.2.2.8 Data Reporting and Visualization

Geometry information is commonly presented in one of two formats: exception reports and foot-by-foot data. Exception reports include all identified anomalies within the inspected area, along with pertinent details such as defect type, length, peak value, severity, safe speed, class drop, GPS coordinates, milepost, and track information. This data is crucial for field personnel tasked with track repairs and ensures compliance with safety standards set by the FRA (2022). Foot-by-foot data are commonly arranged as one row per foot and a corresponding column for each channel described in Section 1.1.2.7.

To graphically display either of the aforementioned reporting methodologies railroads commonly employ a visualization method called a strip chart (Figure 1.9). A strip chart consists of stacked line graphs that share the same x-axis which denotes the location on the tracks (e.g. milepost). The y-axis corresponds to the measurement values for each channel, along with their respective units. Typically, each page of the chart covers a length of only one or two miles, making it easier to read. Each channel can be overlaid with the railroad's specified geometry inspection thresholds. The red threshold corresponds to the current track class. As an example, this could refer to the wide gauge threshold for Class 3 track during a Class 3 track inspection. The yellow threshold represents a class higher than the actual track class. For instance, this could refer to a wide gauge threshold for Class 4 track during a Class 3 track inspection, which is

stricter. This setup enables the railroad to proactively plan maintenance before reaching the red threshold, thereby avoiding speed restrictions that are mandated by the FRA.

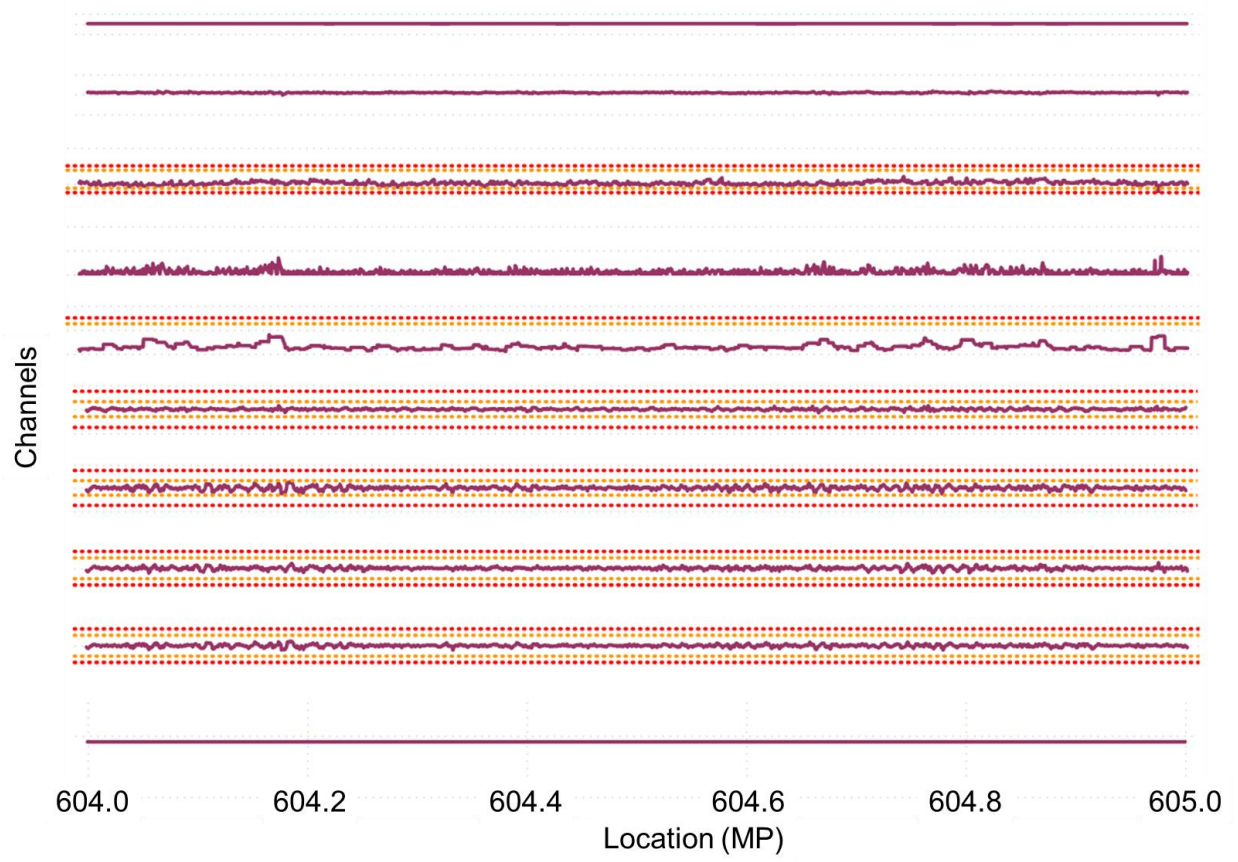

Figure 1.9: Example of a geometry stripchart for a single inspection over one mile of track

Strip charts can also be used to compare two or more geometry inspections at different times by overlaying them in the same graph using different colors (Figure 1.10).

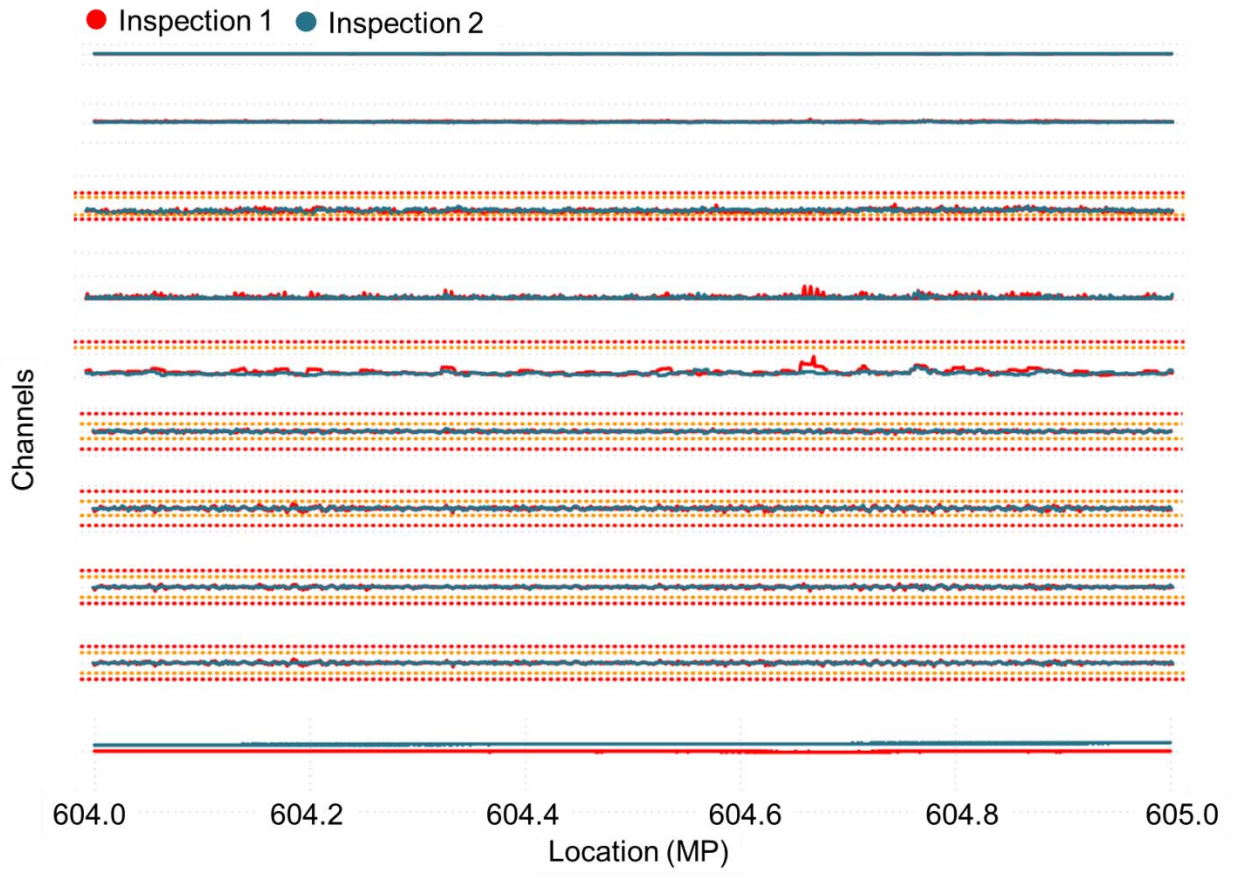

Figure 1.10: Geometry stripchart for two inspections over one mile of track

1.3 Railroad Track Components Considered in this Research

Railroad track is comprised of various components that must function as a system to facilitate the safe and efficient movement of trains. In this study, I focus on crossties, spikes, tie plates, fasteners, ballast, and joint bars using data collected by LR*AI*L. These data included 2D and 3D images of the aforementioned track components to enable height detection. After data were collected, Deep Convolutional Neural Networks (DCNN) process the data to recognize components and evaluate their condition (Harrington et al., 2022). The LR*AI*L system is capable of identifying and rating different component types, such as concrete and timber crossties, cut and screw spikes, and multiple types of tie plates and fasteners.

1.3.1 Data Formats

The LR*AI*L system internally organizes data into two-meter (6.56 feet) by 3.5 meter (11.5 feet) sections. Raw information for each section is stored in Extensible Markup Language (XML) files, which are later parsed into Comma Separated Values (CSV) files. The CSV format was selected for its tabular structure, making it easier to process and store data. Each component has its own CSV file, and these will be described in detail later. Additionally, each section is associated with two images: an intensity image, depicting the laser's reflected intensity to the sensor, and a range image, showing the angle of the reflected laser to the sensor, that is later converted to height. Both images can be overlaid with labels from the DCNN or viewed as seen by the sensors (Figure 1.11). Images are primarily used to validate other system outputs and provide a linear visualization of the track. Point clouds (Figure 1.12) can also be used to verify components that are difficult to be seen in 2D images, such as sunken tie plates and high spikes.

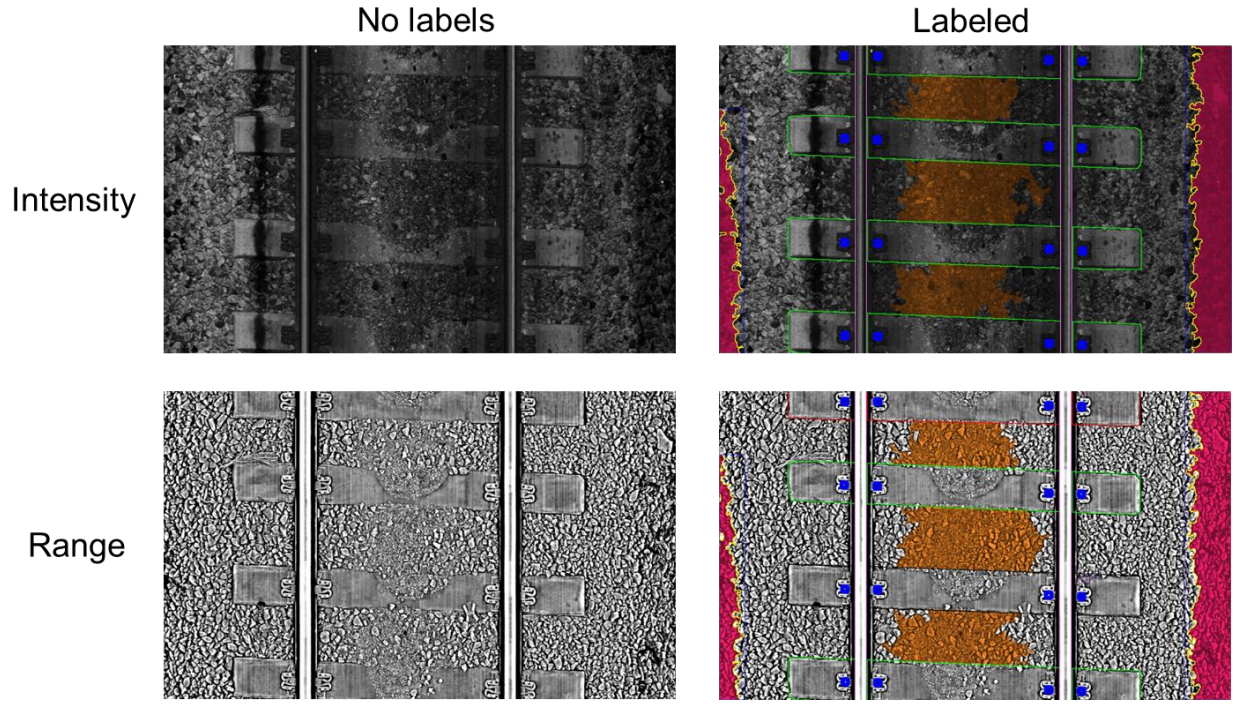

Figure 1.11: Example output images from the LRAIL system and options for data overlay

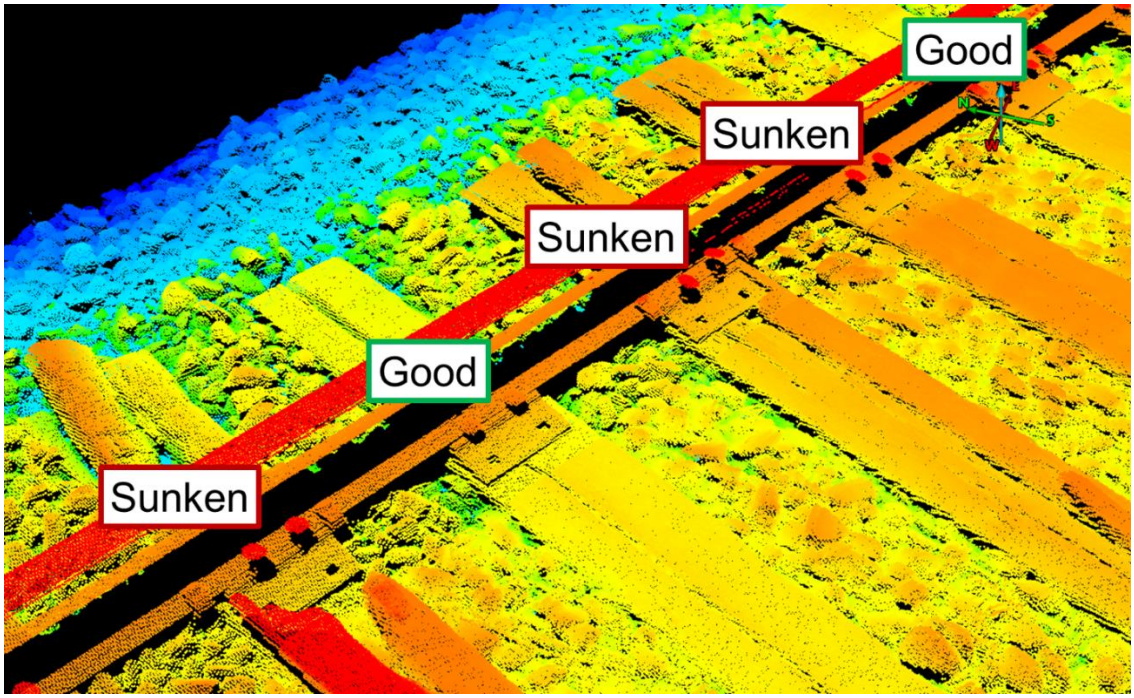

Figure 1.12: Example LR*AI*L 3D point cloud rendering used to assess tie plate condition

For each component, the LR*AI*L system outputs one CSV file, with one row per component identified (Table 1.6). All components are referenced by section, distance (e.g. milepost), and GPS coordinates.

Table 1.6: Relevant data and LR*AI*L outputs for track component inspection

Component	Relevant Data and Measurements
Crosstie	Material, Rating, and Skew angle
Fastener	Type, Condition, and Position
Tie plate	Type, Condition, and Position
Anchor	Type, Condition, Position, and Distance to Crosstie
Spike	Type, Condition, Position, and Height
Joint bars	Length, Number of Bolts, Joint Gap, and Left/Right Rail
Ballast Surface Fouling	Area

Crosstie ratings are calculated using crack length, area, and depth. They are scaled with zero being a good crosstie and two or three being a failed concrete crosstie or timber crosstie, respectively.

LR*AI*L ballast data provides two distinct outputs that are recorded at one-meter (3.2 feet) intervals. The first output, known as the ballast shoulder report, measures the height of the shoulder ballast at predefined distances from the rail (448, 548, 648, 748, and 848 mm; 17.6, 21.6, 25.5, and 33.4 inches). This information can be used to determine the shoulder ballast slope. The second report offers a cross-sectional view of the ballast, with points recorded every eight mm (0.31 inches) from the centerline. These data are used to calculate the variance in ballast quantity within each cross section by comparing it to the design cross section (Figure 1.131.13).

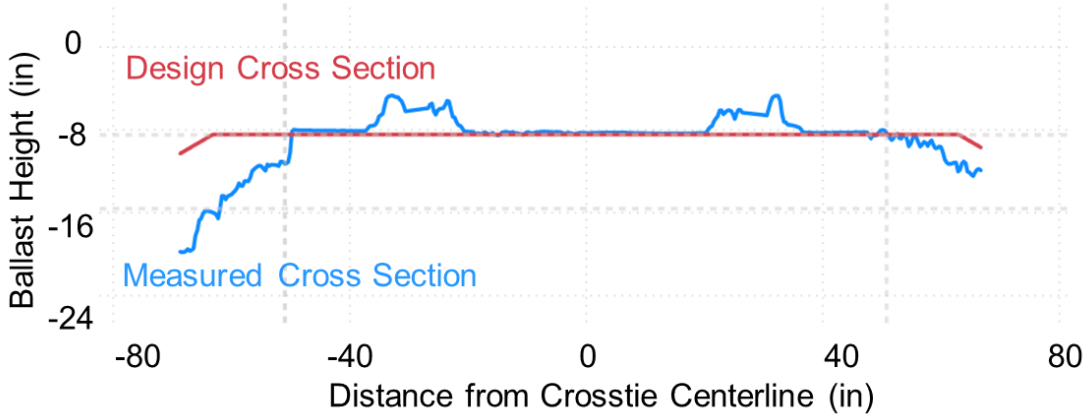

Figure 1.13: Ballast cross section output from LR*AI*L

1.4 Track-related Data within a Railroad Company

The railroad industry has recently begun to embrace the study and use of "big data" due in large part to the vast amount of track inspection data collected. To put this into perspective, Class I railroads operate a total length of 140,000 track miles and conduct an average of two

geometry inspections per year over most of their track, with 5,280 samples collected per mile. This results in the annual collection of approximately 1.5 billion data points, and fails to fully capture additional high-frequency inspections by ATGMS that may occur as often as three times per week. Transforming this massive dataset into meaningful information requires several levels of analysis and processing. In addition to these data, there are other safety-related datasets that include ultrasonic rail flaw, vehicle-track interaction, and rail wear data (Zarembski, 2014).

The levels of data analysis in the railroad industry are commonly related to the company's organizational hierarchy. At the operational level, tasks like corrective maintenance and speed restrictions management require detailed, raw data. Moving up the data use hierarchy to tactical and strategic levels, responsibilities expand to include capital planning and resource allocation over larger areas, like multiple subdivisions, divisions, or the entire network. As we further ascend the organizational structure, the need for intricate data decreases and is replaced by consolidated results derived through multiple data processing steps. The strategic level, which is focused on prioritization of future investments, demands minimal data but requires processing over time for forecasting and trend analysis. Thereby, the strategic level relies on a well-structured data flow from the lower levels. The entirety of the aforementioned data and information generation workflow can be presented as a pyramid (Figure 1.14).

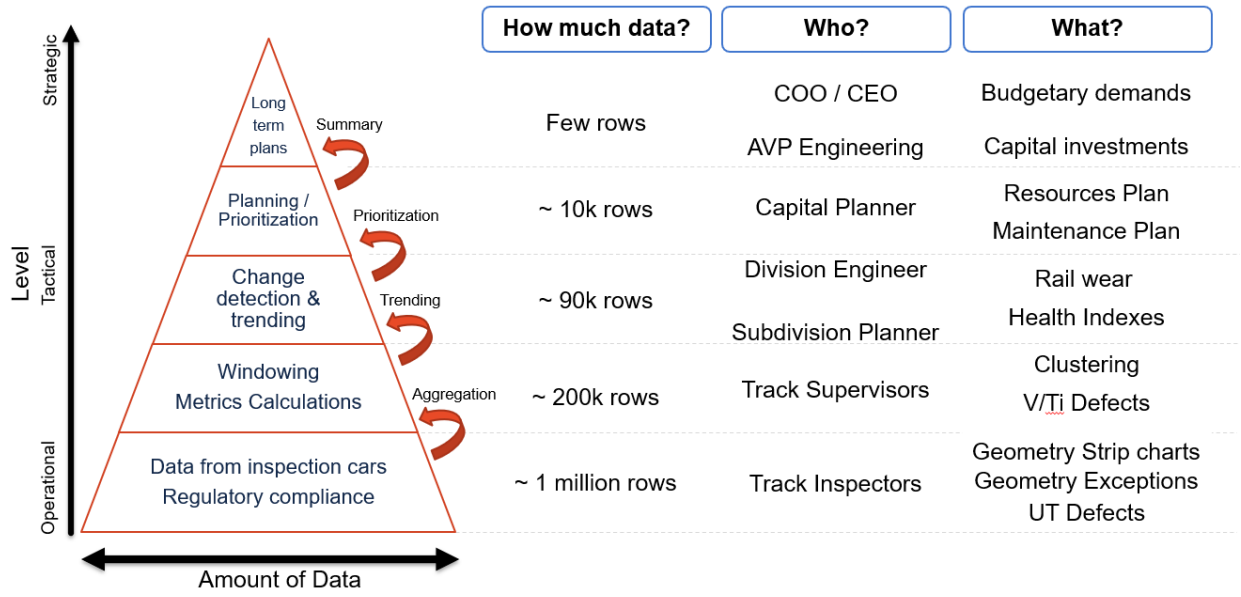

Figure 1.14: Data pyramid and examples of quantity, users, and type of information

The initial analysis involves a check against regulatory requirements, necessitating a thorough evaluation of all data to identify defects or other anomalies. Operational teams utilize these data, which are often presented in strip charts, exception, or defect reports from different sources (e.g. geometry, ultrasonic testing (UT), and vehicle-track interaction (VTI)). Data are commonly used to identify locations that require immediate action such as corrective maintenance or implementing of temporary speed restrictions. Although this dataset covers a long section of tracks, it pertains to shorter sections of the network, thereby making it more manageable and concise for operational teams to interpret and act upon.

At the tactical level, aggregated data is vital for determining resource allocation, including decisions related to crosstie and rail capital replacement operations and capital ballast undercutting jobs. Allocation considerations must account for the broader network-level perspective, factoring in availability and cost-effectiveness. Equally crucial is proper scheduling

of activities through the optimization of resource allocation across the network. This "tactical" dataset comprises rail wear reports, track quality indexes (TQI), and component data.

Strategic levels oversee the entire network, making decisions on capital investments, equipment acquisition, and long-term goals. Despite the grand scale of these decisions, they do not necessitate big data but require concise and summarized datasets. While originating from the lower levels, these data undergo additional processing steps to provide the necessary insights.

Achieving the above objectives within this workflow poses challenges. First, the enormity of data necessitates efficient storage, processing, and visualization methods, often utilizing cloud computing and asset management platforms (Zarembski, 2014). Secondly, the railroad industry as a whole can be slow to adopt new technologies and processes, hindering the acceptance of data-driven decision-making practices. This is due, in part, to how new methods, metrics, and tools integrate with existing FRA inspection requirements. In contrast to other industries, railroads have been slower to establish a robust data pipeline that reaches the highest levels of the pyramid (Figure 1.14). Using the framework provided in this research railroads will be able to process and digest huge amounts of data, collected using state-of-the-art equipment, to provide reliable and safe train movements and communicate to a variety of levels in the railway organizational structure.

CHAPTER 2: INVESTIGATION INTO THE RELATIONSHIP BETWEEN TRACK COMPONENT HEALTH AND TRACK GEOMETRY DATA

2.1 Background

Deviations from design track geometry conditions induce heightened dynamics within the vehicle-track system (Esveld, 2014). These geometry irregularities, which include perturbations to alignment, curvature, elevation, and cross-level, not only affect the movement of trains by causing speed restrictions, but also influence passenger ride quality and accelerate degradation rates of both track geometry and track components (Esveld, 2014).

Every component (e.g. rails, fasteners, crossties, ballast) within the track structure plays a crucial and unique role in maintaining the integrity of the railway track. Rails are the primary structural members upon which trains operate, can experience stress points and wear patterns due to irregular geometry, especially when geometry defects are present, leading to premature deterioration (Zarembski et al., 2016). Crossties support the rails, provide a means of distributing loads to the ballast, anchor the track against movement, and maintain track gauge (through engagement with fastening systems). When crossties wear, decay, or split, they introduce localized instabilities in the track alignment and amplify the overall irregularities in track geometry (Alsahli et al., 2019). Ballast is designed to facilitate drainage and attenuate crosstie loads to a level that can be passed to the subgrade without causing permanent deformation. A lack of ballast can adversely influence track geometry, compromising its effectiveness and leading to instability in the vertical, lateral, and longitudinal directions (Zarembski et al., 2017). Fastening systems (e.g. clips and spikes) secure the rails to the crossties. Misalignments caused by irregular geometry can accelerate fastener deterioration which, if left unaddressed, can lead to heightened derailment risk. Thus, understanding the

relationship between track geometry measurements and the condition of track components is of great importance to infrastructure managers.

Previous studies on crosstie life prediction have made significant strides in development of methods and models for the prioritization of railway track maintenance. Zarembski and Holfeld (1997) developed a model for the prediction of crosstie life using mathematical and statistical methods. Their models considered various track characteristics, including curvature, tonnage, speed, axle load, rail section, and environmental conditions and predicted the lifespan of timber crossties with cut spikes - which represent over 90% of the US railroad network. Soufiane et al. (2022) extended the exploration of crosstie life by investigating how crosstie longevity is affected by adjacent crosstie failures. Their research developed a dynamic machine learning model that considered the gradual deterioration of all crossties as a function of time (Soufiane et al., 2023). Notably, both studies utilized data collected from Aurora®, an automated crosstie inspection tool that is owned and operated by Loram Technologies, Inc.

While these studies provided valuable insight into crosstie health, their focus did not include other components or the interaction of components within the railway track system. Incorporating a broader analysis encompassing all track components could offer a more comprehensive understanding of the railway infrastructure's overall condition, enabling more accurate predictions and targeted maintenance strategies. By integrating data on crossties, ballast, fastenings, and other components into similar predictive models, railways can further improve their ability to ensure safe operations and long track component and system life cycles.

2.2 Introduction

In this chapter, the relationship between geometry and component inspection data will be investigated using statistical approaches. These approaches and applications will be compared across different components using revenue service data from a Class I railroad mainline as the subject test corridor. Unlike previous studies such as in Alsahli et al. (2019), which focused solely on locations with geometry defects, this investigation will encompass a holistic evaluation that is independent of geometry condition and track component heath. Both geometry and component health test data were collected coincident with one another for this research effort.

To facilitate this comparative analysis, the subdivision that was selected for the test corridor will be divided into fixed-length windows of 30 feet (9.14 m) as presented in Section 2.6. Subsequently, an aggregation function will be applied (Section 2.7) that aligns with established FRA track geometry thresholds (Table 1.3). Results from the aggregation functions for each window are then analyzed using a correlation matrix, which allows for the calculation and interpretation of the Spearman correlation index (Daniel, 1990).

It is important to note that this study will focus on the relationship between a single geometry run and a corresponding single component inspection run. This approach aims to capture a snapshot (in the time and tonnage domain) of both geometry conditions and component rating at a specific time step, offering a detailed understanding of their concurrent conditions. Future work will cover the relationship between the degradation of both components as a function of time, using the framework that will be presented in Chapter 3.

2.3 Data Collection

The data for this project was collected over a 115-mile (185 km) section of a Class I railroad subdivision in the southern US. The subdivision is primarily single track with periodic passing sidings and one 10-mile (16 km) double track segment. The route is mostly tangent track with occasional shallow curves and three moderate curves of approximately 6.5 degrees. The line is made up of approximately 72% timber crossties and 28% concrete crossties. The concrete crossties were installed in the 1990's and have either Fastclips or e-clips. The concrete crossties are currently being replaced by timber crossties due to maintenance challenges. Cut spikes are used for most of the timber crossties, with the exception of the 6.5-degree curves which have victor plates and e-clips. Gauge face rail lubricators are used on this corridor. The track is maintained to FRA Track Class 4 and the timetable maximum operating speed for freight trains is 60 miles per hour (96 km/h). There are no regularly scheduled passenger trains operating on the route. The tracks are well maintained and are in good condition overall.

The component inspection data collected for this research were obtained during seven data collection efforts during calendar years 2021-2023. In total, approximately 600 miles (965 km) of data were collected (Table 2.1).

Table 2.1: Component data collection campaigns

Data Collection Campaign (number)	**Collection Date** (month/day/year)	**MP Start** (milepost)	**MP End** (milepost)	**Length** (miles)	**Interval between inspections** (days)
1	12/4/2021	587.99	695.45	107.46	-
2	1/30/2022	587.48	695.56	108.08	57
3	3/18/2022	587.99	683.21	95.22	47
4	6/2/2022	587.98	648.95	60.97	76
	6/3/2022	649.96	685.24	35.28	
5	10/19/2022	587.99	640.39	52.40	139
	10/20/2022	641.02	648.68	7.66	
6	11/17/2022	587.90	694.73	106.83	28
7	6/21/2023	587.97	658.45	70.48	216

At the start of the project the target inspection interval was 60 days. Upon collection, processing, and review of the initial datasets the research team determined that this interval was too short to detect any major changes in the component condition. As such, the inspection interval was increased to allow for more component degradation between consecutive inspection runs.

Geometry data were collected using ATGMS mounted in boxcars operated by the Class I host railroad. This ATGMS boxcar runs on a premium intermodal train that operates over the corridor and passes over the route between two to three times per week. To minimize the large volume of data required for this project, an average interval of 30 days between inspections was selected for down sampling of geometry data. The period of geometry data sampling was from June 2021 to April 2023 and comprised of 24 geometry inspections (Table 2.2). This provided a sufficiently large sample size to facilitate data trending (Section 1.2.1).

Table 2.2: Geometry data collection campaigns

Data Collection Campaign (number)	**Collection Date** (month/day/year)	**MP Start** (milepost)	**MP End** (milepost)	**Length** (miles)	**Interval between inspections** (days)
1	6/6/2021	587.04	697.00	109.96	-
2	7/12/2021	587.04	697.00	109.96	36
3	7/16/2021	586.96	697.00	110.04	4
4	9/12/2021	586.80	663.33	76.53	58
5	10/1/2021	587.00	697.00	110.00	19
6	½/2022	587.01	697.00	109.99	93
7	1/30/2022	586.80	697.00	110.20	28
8	2/8/2022	586.80	697.00	110.20	9
9	2/15/2022	587.00	697.00	110.00	7
10	3/27/2022	600.07	697.00	96.93	40
11	4/6/2022	593.90	695.22	101.31	10
12	4/15/2022	606.14	619.44	13.30	9
13	5/22/2022	586.80	697.00	110.20	37
14	5/26/2022	638.55	696.83	58.28	4
15	6/2/2022	596.89	697.00	100.11	7
16	7/13/2022	586.80	697.00	110.20	41
17	9/19/2022	586.80	697.00	110.20	68
18	10/15/2022	586.80	697.00	110.20	26
19	10/19/2022	586.80	697.00	110.20	4
20	1/30/2023	586.80	697.00	110.20	103
21	2/24/2023	586.80	697.00	110.20	25
22	3/8/2023	586.80	697.00	110.20	12
23	3/10/2023	586.80	697.00	110.20	2
24	4/29/2023	586.80	697.00	110.20	50

Additionally, geometry data from collection runs in close proximity to component inspection runs were selected given the focus of this project is the direct comparison of component heath data and track geometry data. In total, 2,428 miles (3,907 km) of geometry data ware used, made up of 5,280 samples per mile (3,280 per km) and a total data set of 12,824,161 rows.

2.4 Data Processing and Storage

Due to the substantial volume of data generated, processed, and used in this research, local data processing and storage was impractical. In response, a scalable and efficient approach was adopted. All CSV files containing data from both geometry and component inspections were transferred to the Microsoft Azure cloud computing environment. Within Azure, advanced data processing techniques were applied utilizing PySpark notebooks, a powerful tool known for its ability to handle large-scale data processing tasks.

Upon completion of the data processing steps, the refined data was then stored in a more optimized format. Specifically, the processed data were saved as Parquet files, a columnar storage file format that is highly efficient for data analytics purposes. This format not only ensures data integrity but significantly reduces storage space requirements, facilitating effective management and analysis of extensive datasets.

2.5 Data Alignment

The effective alignment of diverse railroad track condition datasets poses a significant challenge. Ensuring seamless comparison across disparate inspection runs and tools, each operating with distinct sample distances, demands sophisticated alignment methodologies. In this project, the use of 30-foot (9.14 m) windows offered a strategy to mitigate the impact of alignment errors over the window's length (Neuhold et al., 2020). It is worth noting that the geometry data, though collected using the same system, often originated from different inspection vehicles. However, alignment accuracy remained consistent due to the uniformity of the location determination systems across different vehicles.

An initial approach for component data alignment involved synchronizing the data with the nearest geometry inspection through Dynamic Time Warping (DTW) as outlined by Palese et al. (2020) based on the GPS coordinates. This method, described theoretically by Salvador and Chan (2007), was initially designed for aligning time-series data for applications such as movement and speech recognition. The DTW algorithm computes the piecewise distance between two signals, generating a distance matrix. Given the computational intensity of this process, cloud computing was imperative. Prior studies explored methods to minimize computational costs by altering signal resolutions and implementing constraints on the matrix size (Xu et al., 2015). DTW operates by finding the shortest path, known as the warping path, between the end points of the signals. This path permits the stretching or shrinking of signals, a critical capability when aligning geometry data prone to errors. The length of this path can be used as a similarity proxy between two signals.

Although the DTW method produced fair alignment between the datasets, there was still room to improve the process with the objective of achieving tie-by-tie alignment between multiple component inspection runs. Since the system outputs the downward images of the tracks, it is possible to identify specific fixed assets (e.g. grade crossings, switch points, and wayside defect detectors) that do not commonly change over time, and relate those with the Positive Train Control (PTC) database provided by the railroad. The PTC database contains the milepost for each asset and is the same database used by the ATGMS for data collection. After identifying these assets, linear interpolation of the milepost is used between assets (Figure 2.1). This procedure yields good results when the distance between fixed assets is small (c.a. less than one mile). However, as the distance increases, the accuracy diminishes.

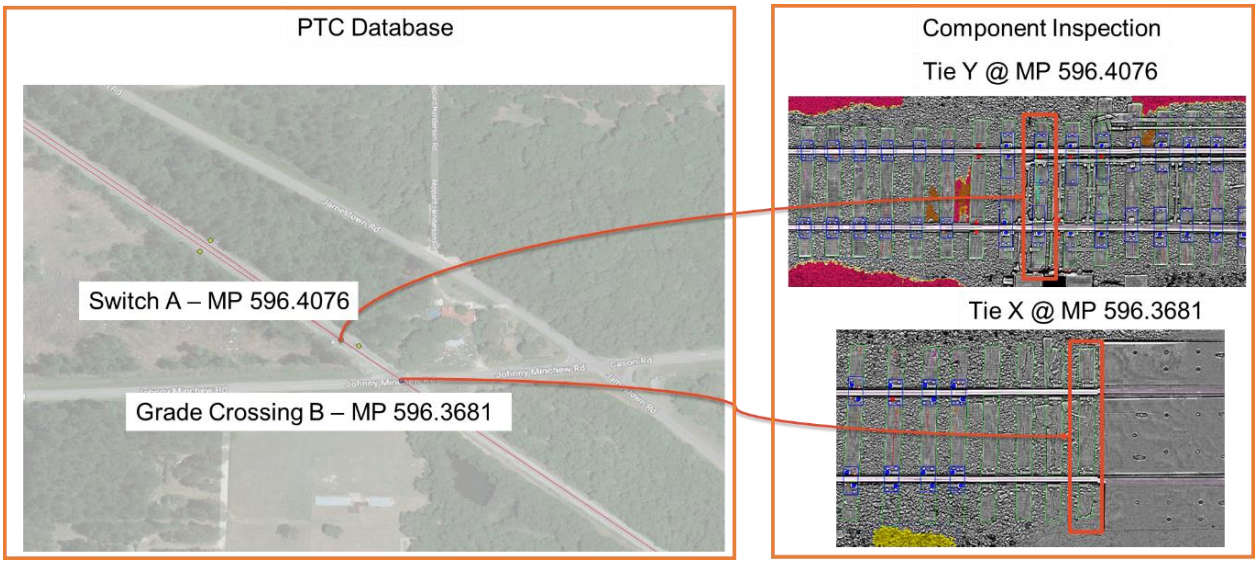

Figure 2.1: Alignment between PTC database location and component inspection data

Future work will apply DTW algorithms between fixed assets in lieu of linear interpolation. This may increase the accuracy of the alignment and is also computationally feasible for locations in which the distance between assets is longer. This is possible given the start and end points match and the warping matrix can be simplified. The longest such distance on our test corridor is approximately three miles long.

2.6 The Windowing Process

Windowing, also known as track segmentation, is a crucial process in railway track analysis in which track is divided into segments with similar characteristics and expected behavior over time (Tzanakakis, 2013). Researchers have employed different strategies for windowing (Table 2.3) and generally aim to strike a balance between accuracy and data availability.

Table 2.3: Track data windowing methods and applications

Research Question	Windowing Interval	Reference
Generic degradation model	Variable, characteristic based	Jovanovic, 2004; Guler et al., 2011; Tzanakakis, 2013
Degradation between tamping cycles	16.4 ft (5 m)	Neuhold et al., 2020
Degradation between tamping cycles	200 ft (60.96 m)	Goodarzi et al., 2020
Different TQI Comparison	328 ft (100 m)	Offenbacher et al., 2020
TQI Development	528 ft (160.9 m)	Sung, 2005
Geometry defects prediction	528 ft (160.9 m)	Sharma et al., 2018
Track quality prediction	984.5 ft (200 m)	Quiroga and Schnieder, 2010
Effects of tamping in track quality	984.5 ft (200 m)	Andrews, 2013
Long term degradation model	1640 ft (500 m)	Fendrich and Fengler, 2019

Researchers have chosen variable window lengths based on factors such as asset characteristics (e.g. curvature, tunnels, bridges, turnouts, crossings), maintenance records (e.g. crosstie and rail type, material, and age), and operational data (e.g. axle load, maximum speed, tonnage). Using asset characteristics provides a nuanced representation of track segments, especially in network-wide studies. However, it demands extensive and specific data, which is not always readily available.

In contrast, other researchers have opted for fixed windows. Fixed windows are predefined segments of consistent length. The advantage of fixed windows lies in the simplicity of data analysis; it reduces the complexity of computations by ensuring uniform segment sizes. This approach is particularly useful when dealing with large datasets, making analysis more manageable.

A combination of both methods is often utilized to capitalize on the advantages of each, provided the necessary data are available. In this hybrid approach, fixed windows are employed, and each window is tagged with information indicating its specific characteristics (e.g. whether it is a tunnel, switch, or a specific crosstie type). This hybrid method leverages the simplicity of fixed windows while incorporating detailed information about each segment, thus offering a balanced approach to track segmentation and data analysis.

Shorter windows ranging from 31 to 62 feet (10 to 20 meters) are commonly used for generating detailed maintenance plans for execution by local track maintenance forces (Jovanovic, 2004). These shorter windows allow precise analyses and are instrumental in the scheduling of tamping activities. Longer windows ranging from 1,640 to 3,280 feet (500 to 1000 meters) are useful for budgeting and long-term prediction on the order of 30 to 50 years (Guler et al., 2011). Additionally, even longer sections spanning 3.1 to 12.5 miles (5 to 20 km) are employed for planning the deployment of large capital maintenance equipment such as ballast undercutters or track renewal machines, as well as for conducting network-wide assessments (Guler et al., 2011).

The selection of an appropriate window length is crucial to the modeling process and should align with the specific research objectives and hypotheses under investigation. Opting for longer windows (e.g. 52.8 feet (16.1 meters)) results in larger sections containing approximately

30 crossties, potentially diluting the impact of defective components within that window. Choosing a 30-foot (9.14 meter) window reduces the number of crossties to 18, intensifying the influence of defective components compared to a longer window. To best achieve the objectives of this research, a shorter fixed window of 30 feet (9.14 meters) was chosen to ensure a more pronounced effect of defective components.

Additionally, the windowing process plays a role in addressing the challenges posed by poorly aligned datasets (Neuhold et al., 2020). Even if two data collection runs remain misaligned after the alignment process outlined in Section 2.4, as long as the error falls within the window length, it does not pose a significant issue. In contrast, execution of a sample-by-sample analysis necessitates perfect alignment of foot-by-foot data which requires substantial time and effort. The appropriate and strategic use of windows can alleviate the burden of achieving precise alignment, thereby ensuring more efficient data analysis.

The use of fixed windows offers several advantages in the analysis of continuous data (e.g. geometry, rail wear, and component health). Breaking down continuous datasets into discrete segments significantly reduces the volume of data thus making it more manageable for analysis. Additionally, fixed windows enable the comparison of datasets collected at different sampling rates, a common challenge encountered when comparing different track-focused datasets. For instance, geometry data are typically collected every foot, while component data are organized on a crosstie-by-crosstie basis (as explained in Chapter 1). With a crosstie spacing of 20 inches (50.8 cm), each crosstie would be associated with one or two geometry samples. This would require a very precise alignment technique between two datasets captured with different sampling rates, the complexity of which falls outside the scope of this research. In summary, applying the same fixed windowing process to both datasets reduces the need for meticulous

alignment, standardizes the data, and organizes it in a manner that facilitates comparative analyses.

2.7 The Data Aggregation Function

To effectively reduce the amount of continuous data generated, it is necessary to apply a function that takes the continuous data for each window and outputs a single representative value for each window. This is referred to as an aggregation function (Table 2.4), which can be developed to map to the required thresholds imposed by the FRA (Table 1.3).

Table 2.4: Aggregation functions for track inspection parameters

Inspection Type	Parameter	Aggregation Function	Threshold defined by the FRA?
Geometry	Gauge	Maximum	Yes
	Twist/Warp	Maximum of the absolute value	Yes
	Alignment**	Maximum, Minimum and Standard Deviation	Yes, maximum and minimum
	Profile**	Maximum, Minimum and Standard Deviation	Yes, maximum and minimum
	TQI	Maximum	No
	Crosslevel	Average	Yes*
Component	Superficial Fouling	Sum	No
	Defective Crossties	Count	Yes*
	% of Defective Crossties	Normalization****	No
	Crosstie Rating	Average	No
	Weighted Crosstie Rating***	Maximum	No
	Defective Fasteners	Count	No
	% of Defective Fasteners	Normalization****	No
	Defective Tie Plates	Count	No
	% of Defective Tie Plates	Normalization****	No
	Defective Spikes	Count	No
	% of Defective Spikes	Normalization****	No

* Not directly defined.
** Both sides (left and right) for 62' chord length and space curve channels.
*** As defined by Alsahli et al. (2019).
**** Dividing the number of defective components by the total number of that component in the window.

Through the application of an aggregation function the trending framework can be used to predict when a geometry defect will occur within a given window. The aggregation function can also be related to track quality. Track Quality Index (TQI) is a broad term used to describe a mathematical relationship that describes the overall quality of track. The most commonly

accepted and used TQI is the average standard deviation of profile (Audley and Andrews, 2013; Offenbacher et al., 2020), which is a measure of the roughness of the track in a certain location.

Each measured parameter can have one or multiple aggregation functions applied to it depending on the purpose of the analysis. For gauge measurements, for example, the aggregation function can be the maximum value within each window. A maximum value works well for aggregating data given gauge degradation leads to wider gauge and the value increases in the positive direction as a function of time. In the case of twist and warp measurements, which can take on either positive or negative values, the maximum function should be combined with an absolute value function since there is no practical difference between positive and negative values. For measurements that can have positive and negative values that indicate degradation of interest, such as alignment and profile, both maximum and minimum functions should be applied. For some specific measurements, such as cross level and rail wear the average value can be returned. Twenty seven unique geometry parameters were studied in this research.

For component inspection data, which are captured at a sampling rate lower than what is used for geometry, a simple counting function can be used. For example, counting the number of defective crossties in a certain window or the average condition of the crossties (Alsahli et al., 2019) and considering the range from 1 (good) to 3 (defective). One could also consider the number of a specific model of fasteners to provide an inventory of different systems. Simply counting the defective components makes the aggregated data easy to interpret for field personnel that may need to inspect that section prior to planning and executing maintenance. The number of defective components can be divided by the total number of that specific type of

component to obtain a normalized (percentage) number of defective components in that section. In this research effort I will study 11 component inspection parameters.

The influence length of a TQI plays an important role in its calculation. TQIs can be calculated using either moving or fixed windows. By using moving windows, the calculations are influenced less by bad spots and the number of samples are not reduced. Thus, for every sample there will be an associated TQI calculated, increasing required memory and computational costs. On the other hand, when using fixed-length windows, if there is a problem on the border of two windows, both windows will be marked as a defect thus increasing the length identified for maintenance (Neuhold et al., 2020). To mitigate this effect the TQI used in my research will be calculated using a 200 feet (60 m) moving window (Goodarzi et al., 2020) (Equation 2.1). Subsequent to that, the maximum over the fixed 30 feet (9.14 m) window will also be calculated.

$$TQI = \mathrm{MAX}(SD\left(\frac{Profile_{Left} + Profile_{Right}}{2}\right)_{over\ 200\ feet})_{over\ 30\ feet} \qquad \text{Eq. 2.1}$$

2.8 Methodology

For each 30 ft (9.14 m) window, both of the aforementioned component and geometry metrics were calculated and then compared. This process was repeated for all combinations of runs to account for different stages of degradation and maintenance cycles. Images generated by LR*AI*L were used to validate component condition. Scatter plots and correlation matrices, using the Spearman correlation index, were also used to identify relationships.

2.9 Crosstie Condition

The first step in the analysis of crosstie condition is to check for gauge defects. There were very few geometry defects in all datasets from the test section, showing that this subdivision is well-maintained. In one location of tangent track constructed with concrete crossties, a yellow tag wide gauge defect (e.g. one class higher) was found with a maximum value of 0.86 in (21.8 mm) (Figure 2.2). This condition is not yet a concern for the railroad, since the safety (red) threshold was not reached, but maintenance in this location should be planned.

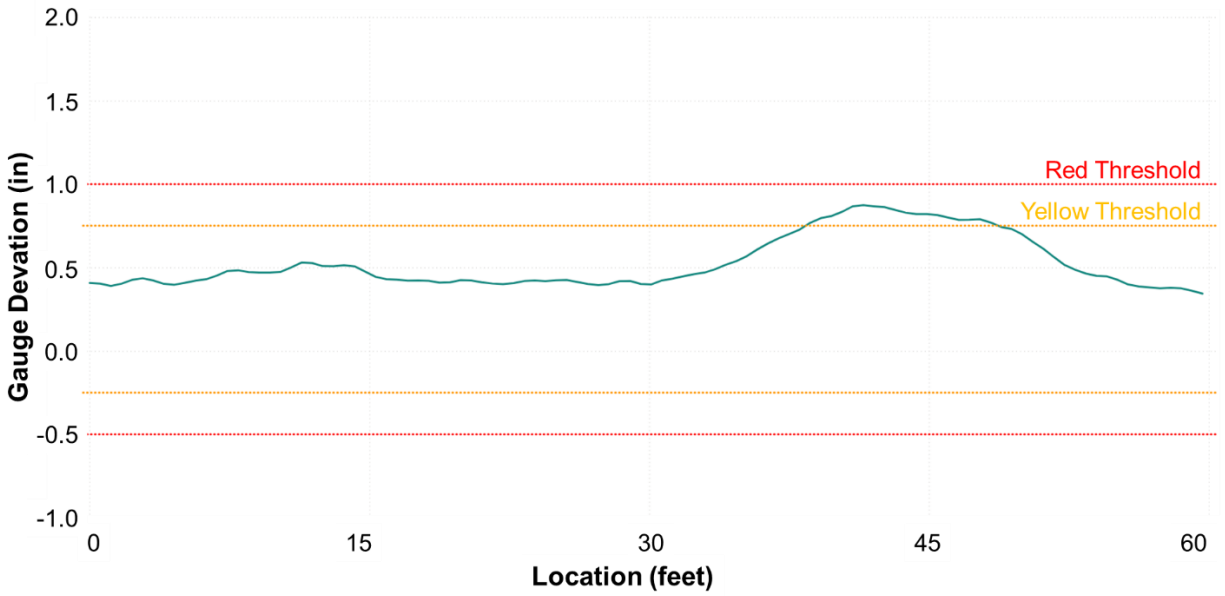

Figure 2.2: Gauge strip chart for the first example window

The crosstie condition was assessed using the metrics described in Section 2.7. There were 15 concrete crossties within this zone, four of which were marked as defective (condition two, black bounding box) and three were identified as poor (condition one, bounding box red). The remaining eight crossties were marked as good (condition zero, bounding box green). A summary of the crosstie metrics for this section is provided in Table 2.5.

Table 2.5: Crosstie metrics for the first example window

Number of defective crossties	Normalized defective crossties (%)	Average crosstie rating	Weighted crosstie rating
4	26.67	1.73	2.15

By checking the images for this section (Figure 2.3), it is noteworthy that the failed crossties are not in sequence – a condition common for a wide gauge defect. In fact, every fifth crosstie has been intentionally broken to support a capital replacement strategy driven by the company, which has no effect on the safety for this section.

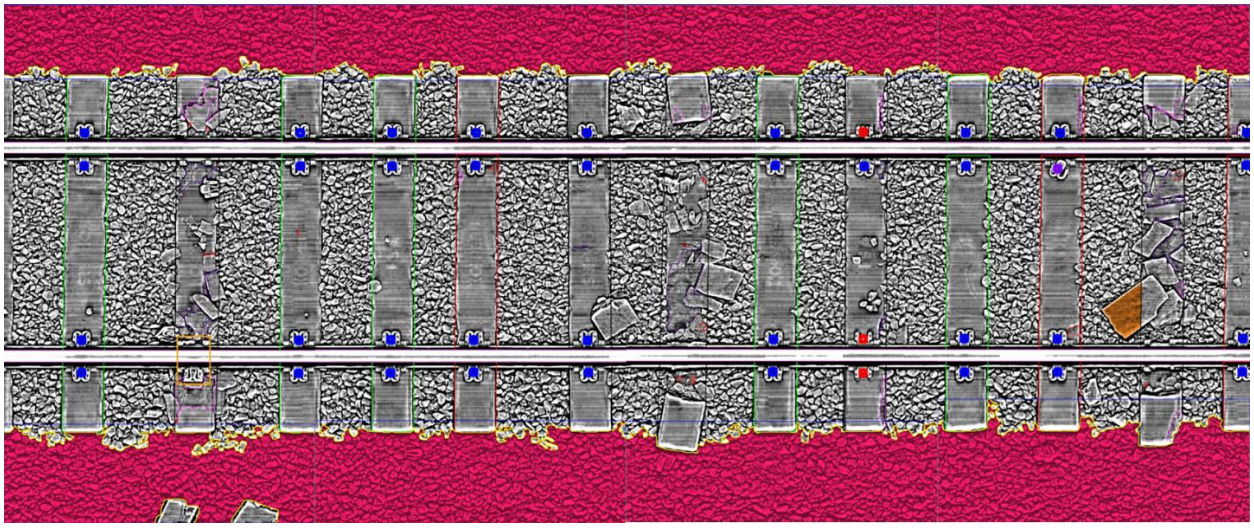

Figure 2.3: Range images for the first example window

In another section containing a 6.75-degree curve constructed with timber crossties, a red tag wide gauge defect was found with a maximum value of 1.26 inches (32 mm) (Figure 2.4). In this location, no failed crossties were found and the overall condition is very good, although some contaminated ballast is present (Figure 2.5).

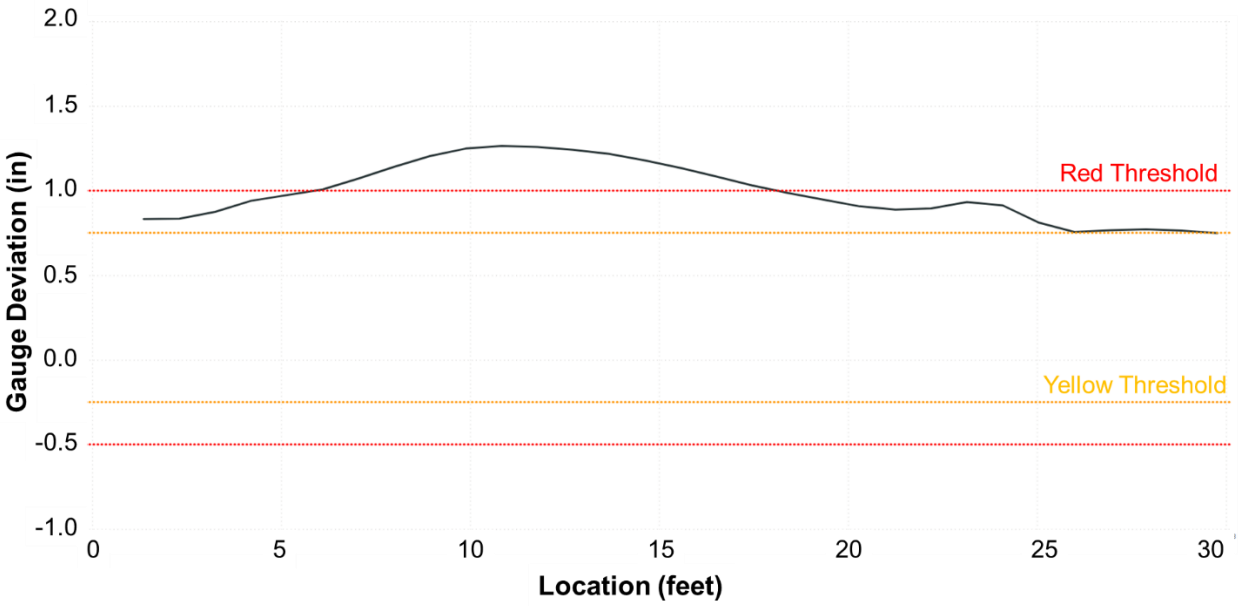

Figure 2.4: Gauge strip chart for the second example window

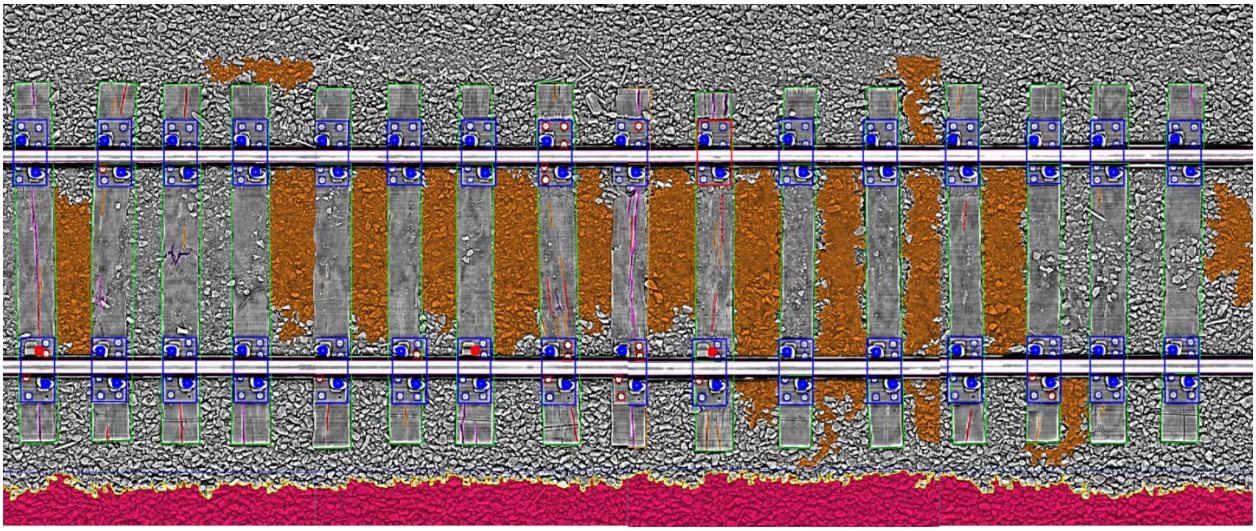

Figure 2.5: Range images for the second example window

These two example locations reveal that – even when there is a geometry defect – the crosstie condition can still be good. The opposite is also true – when the crossties are degraded – the geometry may not have a FRA geometry defect. This trend is observed throughout the entire

dataset when reviewing results from other variables. The scatter plot (Figure 2.6) shows no visible relationship between maximum wide gauge and average crosstie rating. The correlation matrix (Table 2.6: Correlation matrix for) also does not show any relevant number for other variables.

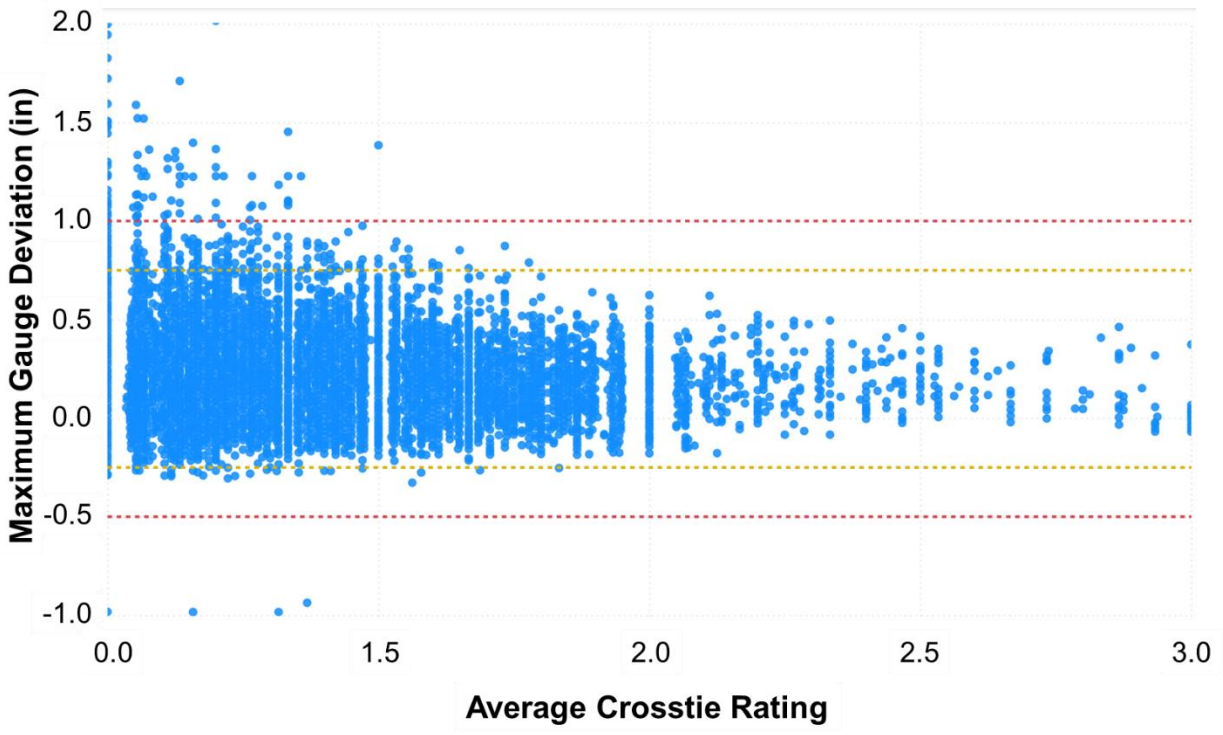

Figure 2.6: Scatter plot maximum gauge and average crosstie rating per window

Table 2.6: Correlation matrix for crosstie data

Geometry Parameter	Number of Defective Ties	Average Crosstie Rating	Normalized Defective Crossties (%)	Weighted Crosstie Rating
Max Gauge	0.06	0.03	0.06	0.04
Min Left Profile 62	-0.07	-0.02	-0.07	-0.02
Max Left Profile 62	0.06	0.01	0.06	0.02
Min Right Profile 62	-0.07	-0.01	-0.07	-0.02
Max Right Profile 62	0.06	0.01	0.06	0.01
Min Left Profile Space Curve	-0.05	-0.03	-0.05	-0.03
Max Left Profile Space Curve	0.00	0.00	0.00	0.00
Min Right Profile Space Curve	-0.06	-0.03	-0.06	-0.03
Max Right Profile Space Curve	0.00	0.00	0.00	0.00
Min Left Alignment 62	-0.01	-0.01	-0.01	-0.02
Max Left Alignment 62	0.01	0.01	0.01	0.02
Min Right Alignment 62	-0.02	0.00	-0.02	-0.01
Max Right Alignment 62	0.01	0.00	0.01	0.00
Min Left Alignment Space Curve	-0.01	0.00	-0.01	0.00
Max Left Alignment Space Curve	0.00	-0.01	0.00	-0.01
Min Right Alignment Space Curve	-0.01	0.00	-0.01	0.00
Max Right Alignment Space Curve	0.00	-0.01	0.00	-0.01
Max TQI	0.07	0.04	0.08	0.05
Max Std. Mean Alignment	-0.01	0.00	-0.02	0.01
Max Std. Left Profile 62	0.07	0.04	0.07	0.05
Max Std. Right Profile 62	0.08	0.03	0.08	0.04
Max Std. Left Alignment 62	-0.01	0.02	-0.01	0.03
Max Std. Right Alignment 62	-0.01	0.01	-0.01	0.02
Average Cross Level	0.01	0.01	0.01	0.01
Average Curvature	0.00	-0.01	0.00	-0.01
Max Twist 31	0.06	-0.03	0.06	-0.03
Max Warp 62	0.07	-0.04	0.07	-0.03
Normalized Gauge	0.06	0.03	0.06	0.04

2.10 Fastener Condition

Defective fasteners can lead to wide gauge, poor rail (roll over) restraint, and Rail Seat Deterioration (RSD). While traditional track geometry systems can quantity gauge and gauge deviations, rail restraint and RSD are best quantified by measuring rail cant or through the use of

a Gauge Restraint Measurement System (GRMS). No GRMS or rail cant data were available for our test section, thus wide gauge will be used as a geometry-based proxy for fastener condition.

In the example section of tangent track constructed of concrete crossties and Fastclips shown in Figure 2.7 there are 61 fasteners identified by the LR*AI*L system. Seventeen were identified as loose (purple marker) and the remaining 44 were found to be in good condition (blue marker). The loose fasteners are primarily located on the gauge side of right rail (bottom portion of Figure 2.7).

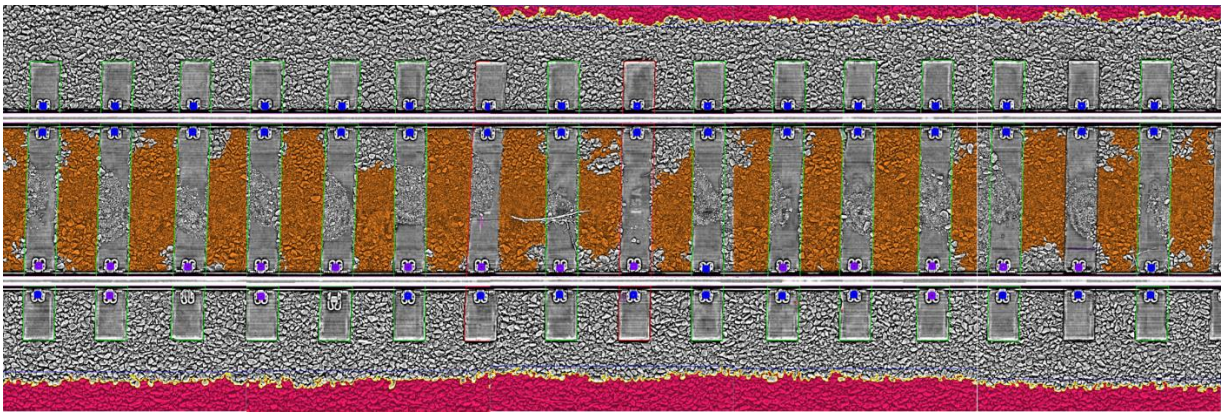

Figure 2.7: Range images for section with defective fasteners

The strip chart for this section (Figure 2.8) does not show any relevant gauge deviation, although the gauge seems to have high variation over a relatively a short distance.

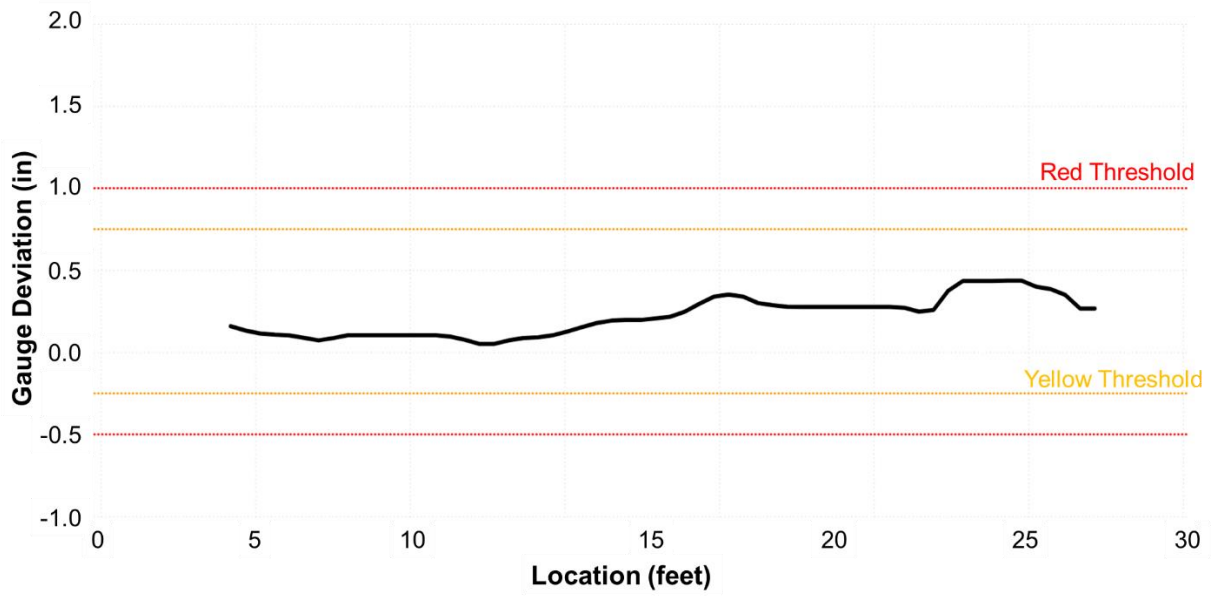

Figure 2.8: Strip chart for the section with defective fasteners

The scatter plot of maximum gauge and normalized defective fasteners (Figure 2.9) do not present any obvious relationship.

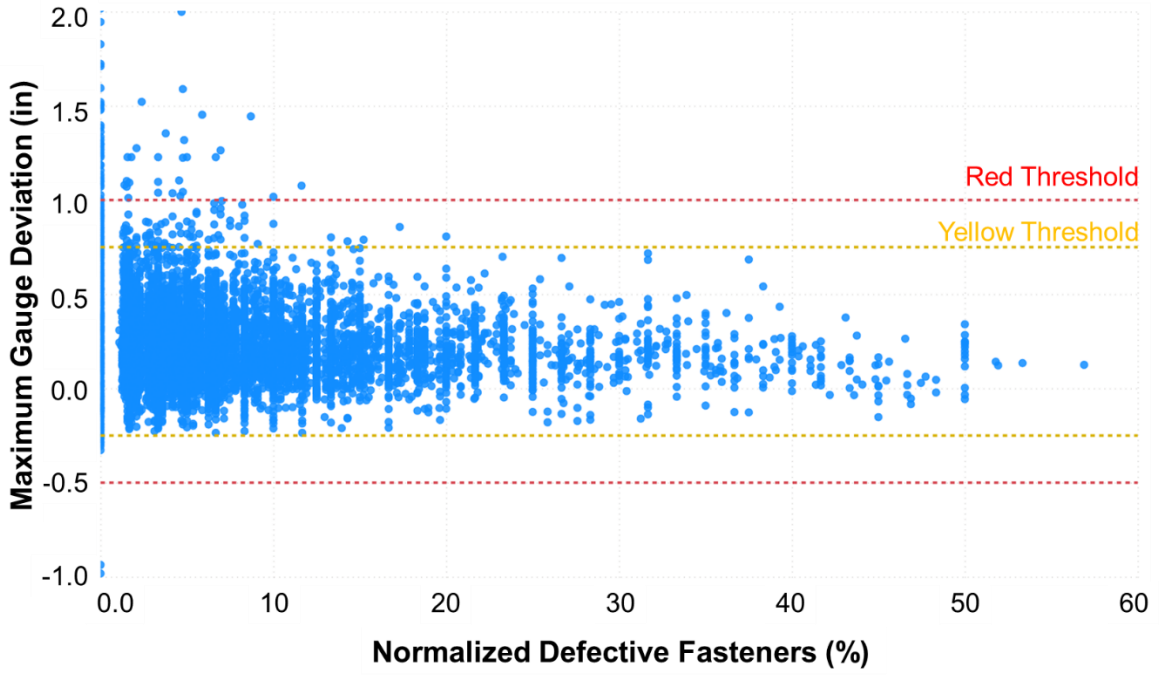

Figure 2.9: Scatter plot of normalized defective fasteners and maximum gauge deviation

The correlation matrix (Table 2.7) also fails to reveal a correlation with other parameters as all of the values are close to zero. Higher values (closer to 1 or -1) indicate stronger correlations. Positive values show direct correlation (e.g. both parameters are getting positive or negative together) and negative values presents inverse correlation (e.g. one parameter gets more positive and the other one gets more negative).

Table 2.7: Correlation matrix for fastener data

Geometry Parameter	Number of Defective Fasteners	Normalized Defective Fasteners (%)
Max Gauge	0.09	0.08
Min Left Profile 62	-0.07	-0.06
Max Left Profile 62	0.07	0.05
Min Right Profile 62	-0.07	-0.06
Max Right Profile 62	0.07	0.06
Min Left Profile Space Curve	-0.03	-0.03
Max Left Profile Space Curve	0.03	0.02
Min Right Profile Space Curve	-0.03	-0.03
Max Right Profile Space Curve	0.04	0.02
Min Left Alignment 62	-0.05	-0.04
Max Left Alignment 62	0.05	0.04
Min Right Alignment 62	-0.05	-0.04
Max Right Alignment 62	0.05	0.04
Min Left Alignment Space Curve	-0.02	-0.02
Max Left Alignment Space Curve	0.00	0.00
Min Right Alignment Space Curve	-0.03	-0.02
Max Right Alignment Space Curve	0.00	0.00
Max TQI	0.09	0.08
Max Std. Mean Alignment	0.04	0.03
Max Std. Left Profile 62	0.09	0.07
Max Std. Right Profile 62	0.09	0.08
Max Std. Left Alignment 62	0.04	0.04
Max Std. Right Alignment 62	0.04	0.04
Average Cross Level	-0.01	-0.02
Average Curvature	0.00	-0.01
Max Twist 31	0.07	0.06
Max Warp 62	0.08	0.07
Normalized Gauge	0.09	0.08

2.11 Tie Plate Condition

Tie plates are components within the track system that support the rails and distribute loads to the crossties at a level that should not exceed the compressive strength of the timber, thereby avoiding plate cutting. Their condition is mostly assessed through rail cant which identifies plate cutting, and lateral tie plate movement can be assessed using GRMS. In the case that neither type of data are available wide gauge may be used as a proxy if it is collected under load.

Figure 2.10 is an example window of 19 timber crossties on tangent track that is located approximately 13 ft (4 m) from a highway-rail grade crossing. It contains 15 defective tie plates, most of them sunken (red bounding box) resulting in 37.5% normalized defective tie plates. The example section also has three failed crossties (condition three, black bounding box), two in fair condition (condition two, red bounding box), and the remaining 15 crossties are good (condition one, green bounding box). The average rating of the 19 crossties within this window is 2.15.

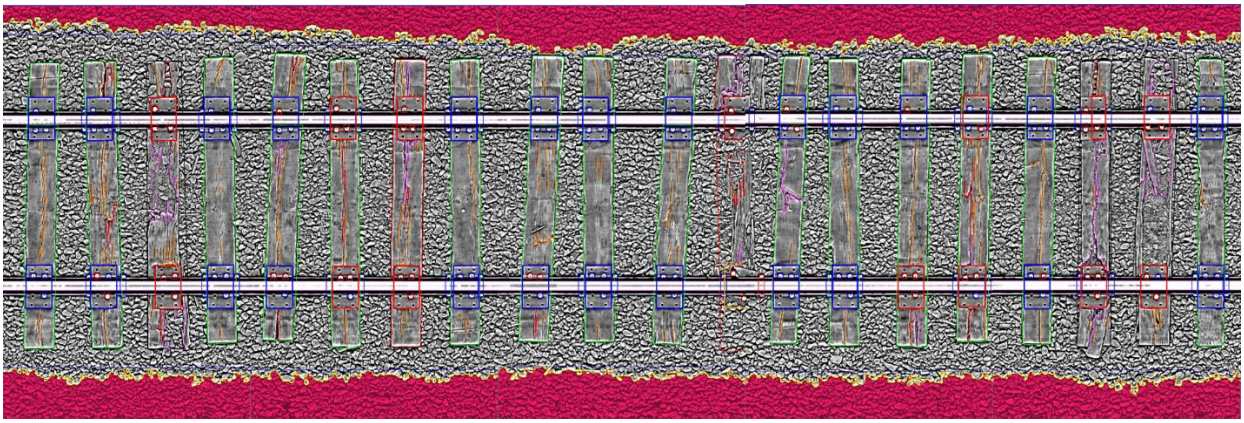

Figure 2.10: Example window for tie plate condition

Although some defective crossties are present, the maximum gauge deviation found in the window is 0.22 in (5.6 mm). This may be explained by the fact that even sunken tie plates are capable of holding gauge. However, since it is a section of tangent track, there is not enough

lateral force to cause gauge widening of a magnitude that is measurable by the ATGMS boxcar. The scatter plot (Figure 2.11) and the correlation matrix (Table 2.8) also do not show any explicit correlation.

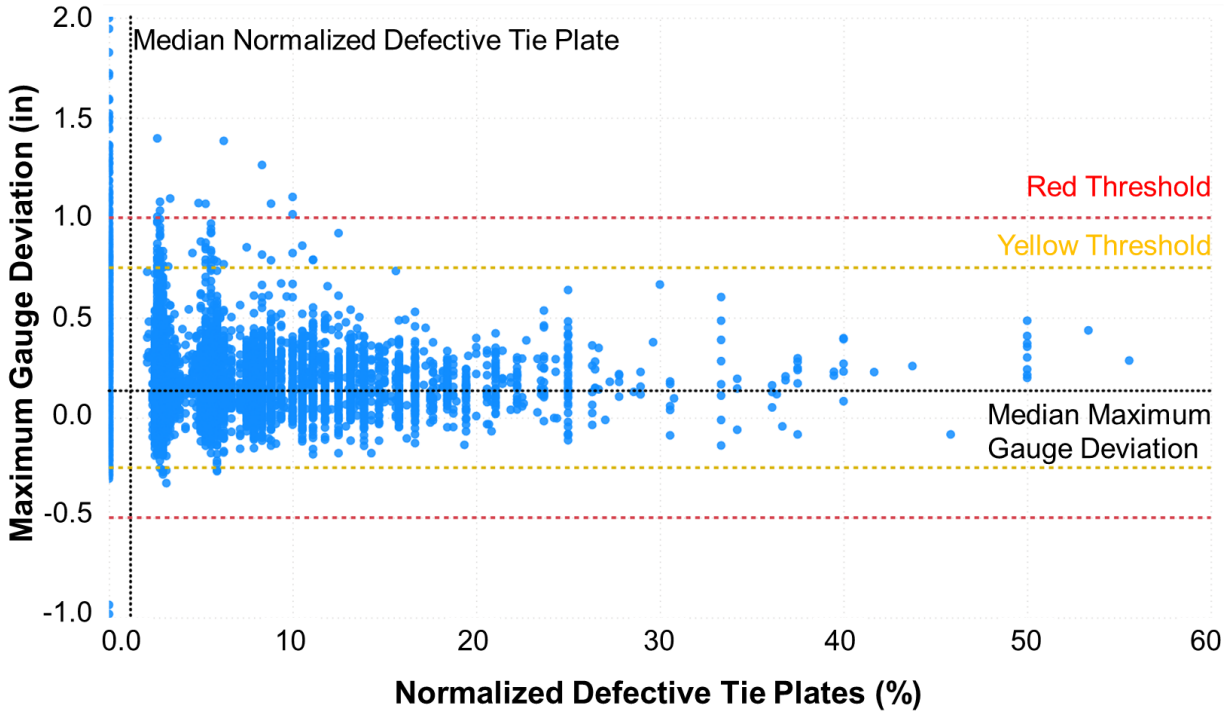

Figure 2.11: Scatter plot of maximum gauge deviation and normalized defective tie plates

Table 2.8: Correlation matrix for tie plate data

Geometry Parameter	Number of Defective Tie Plates	Normalized Defective Tie Plates (%)
Max Gauge	0.01	0.02
Min Left Profile 62	-0.02	-0.04
Max Left Profile 62	0.01	0.03
Min Right Profile 62	-0.01	-0.03
Max Right Profile 62	0.00	0.02
Min Left Profile Space Curve	-0.02	-0.03
Max Left Profile Space Curve	0.00	0.01
Min Right Profile Space Curve	-0.01	-0.02
Max Right Profile Space Curve	0.00	0.00
Min Left Alignment 62	-0.01	-0.01
Max Left Alignment 62	0.02	0.02
Min Right Alignment 62	0.00	0.00
Max Right Alignment 62	0.00	0.00
Min Left Alignment Space Curve	0.00	0.00
Max Left Alignment Space Curve	0.00	0.01
Min Right Alignment Space Curve	0.00	0.00
Max Right Alignment Space Curve	0.00	0.00
Max TQI	0.05	0.07
Max Std. Mean Alignment	0.03	0.03
Max Std. Left Profile 62	0.04	0.07
Max Std. Right Profile 62	0.03	0.05
Max Std. Left Alignment 62	0.05	0.05
Max Std. Right Alignment 62	0.03	0.04
Average Cross Level	0.00	0.00
Average Curvature	0.00	0.00
Max Twist 31	-0.02	0.00
Max Warp 62	-0.02	0.00
Normalized Gauge	0.01	0.02

2.12 Cut and Screw Spike Condition

Cut and screw spikes are track components that hold down both the tie plate and the rails. They can be either driven or screwed into the crosstie. Uplift of the rails causes the spikes to

loosen, which lessens contact between the rail and tie plate and reduces the restraint of the rail. When spikes break due to high longitudinal stresses the fracture surface is commonly around 1.5 in (38.1 mm) below the top of the crosstie surface, making these defects difficult to detect (Roadcap et al., 2019). Currently, none of the commercially available track inspection systems can detect this failure mode. However, using a 3D inspection system that is capable of detecting height can give some information on the health of the spikes. The threshold for a spike to be considered defective (due to being raised) is 1 in (25 mm) above the surface of the tie plate.

The example window in Figure 2.12 is timber crosstie track located on a ballasted deck bridge at the transition from concrete crossties. There are 99 defective (high) spikes in this section (almost 79% of all spikes) and only three defective crossties. The track gauge does not show any abnormal values other than being slightly tight toward the end of the bridge (Figure 2.13). Additionally, there were no visible relationships observed in the scatter plot (Figure 2.14) and correlation matrix (Table 2.9).

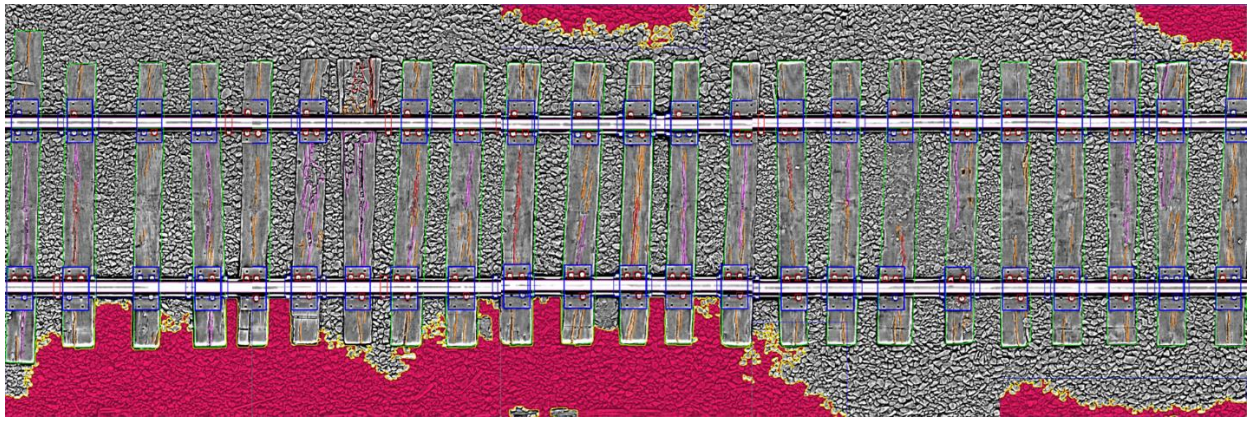

Figure 2.12: Example window for defective spikes

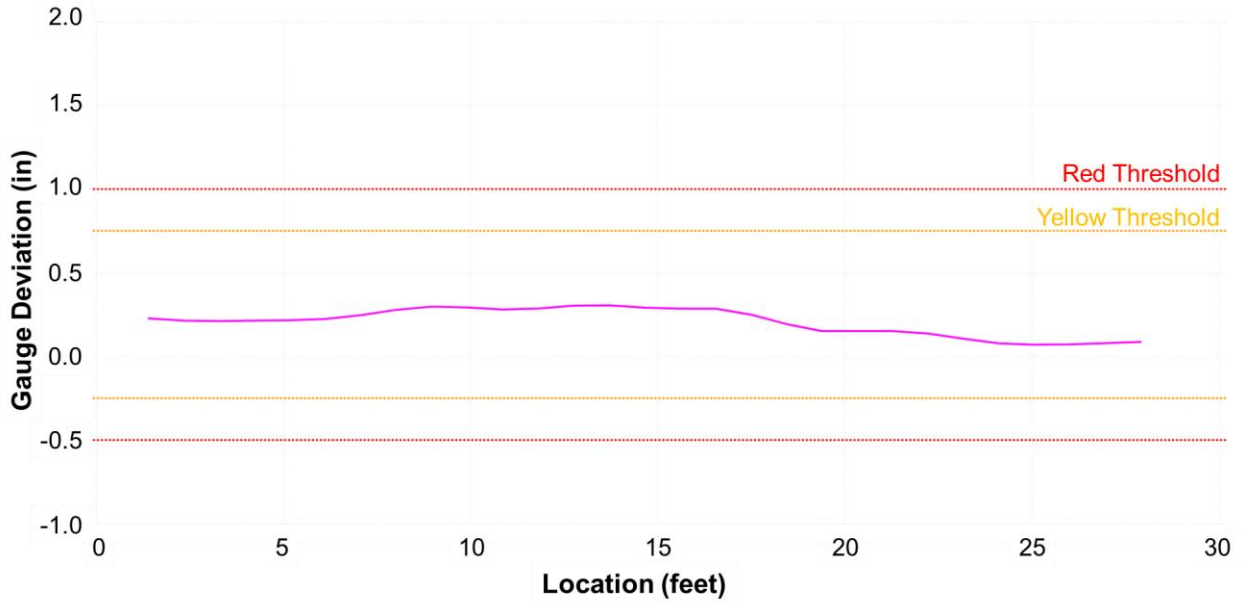

Figure 2.13: Strip chart for the section with defective spikes

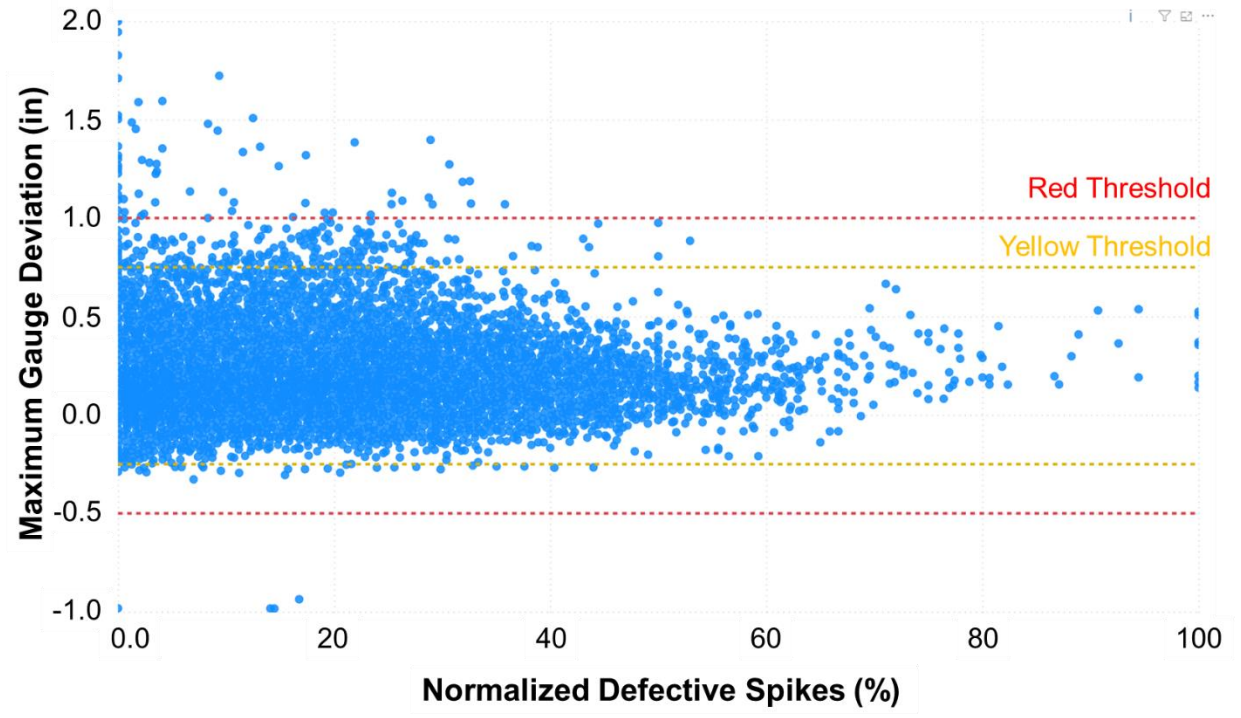

Figure 2.14: Scatter plot of maximum gauge deviation and normalized defective spikes

Table 2.9: Correlation matrix for spike data

Geometry Parameter	Number of Defective Spikes	Normalized Defective Spikes (%)
Max Gauge	0.00	-0.01
Min Left Profile 62	0.00	-0.03
Max Left Profile 62	0.00	0.02
Min Right Profile 62	0.00	-0.03
Max Right Profile 62	-0.01	0.02
Min Left Profile Space Curve	-0.02	-0.03
Max Left Profile Space Curve	0.00	0.02
Min Right Profile Space Curve	-0.02	-0.02
Max Right Profile Space Curve	0.00	0.01
Min Left Alignment 62	-0.03	-0.03
Max Left Alignment 62	0.03	0.03
Min Right Alignment 62	-0.01	-0.02
Max Right Alignment 62	0.02	0.02
Min Left Alignment Space Curve	0.01	0.01
Max Left Alignment Space Curve	0.00	0.00
Min Right Alignment Space Curve	0.01	0.01
Max Right Alignment Space Curve	0.00	0.00
Max TQI	0.06	0.10
Max Std. Mean Alignment	0.08	0.08
Max Std. Left Profile 62	0.06	0.09
Max Std. Right Profile 62	0.05	0.08
Max Std. Left Alignment 62	0.10	0.10
Max Std. Right Alignment 62	0.08	0.08
Average Cross Level	0.02	0.02
Average Curvature	0.02	0.01
Max Twist 31	-0.03	-0.01
Max Warp 62	-0.03	-0.02
Normalized Gauge	0.00	-0.01

2.13 Rail Anchor Condition

The primary function of rail anchors is to restrain the rails from moving longitudinally through engagement with the side of the crosstie. Anchors are most commonly used with timber

crossties and cut spikes given these systems have negligible longitudinal restraint absent anchors. Proper anchor function requires engagement with the side of the crosstie. If they are not, and there is a gap between the crosstie and anchor, they will not provide restraint until the crosstie is displaced enough to engage the anchor. Therefore, the metric used to rate anchor performance is the distance between anchor and crosstie. If this distance is more than 12 mm (0.47 in) the anchor is considered defective.

The example section of track shown in Figure 2.15 is constructed of timber crossties, cut spikes, and anchors that are applied to each side of all crossties (fully box anchored). The section is approximately 31 ft (10 m) from the facing point direction of a turnout, which explains the box anchoring based on typical railroad maintenance practices. Outside of locations with high longitudinal stiffness such as turnouts and grade crossings, it is more common for every other crosstie to be anchored. There are 18 crossties, none of which are defective. Out of the 83 anchors in this section, 32 are defective (38%). All of the defective anchors are located on the left side of the crosstie, which may indicate that the rails are moving in that direction. There are no geometry defects in this window.

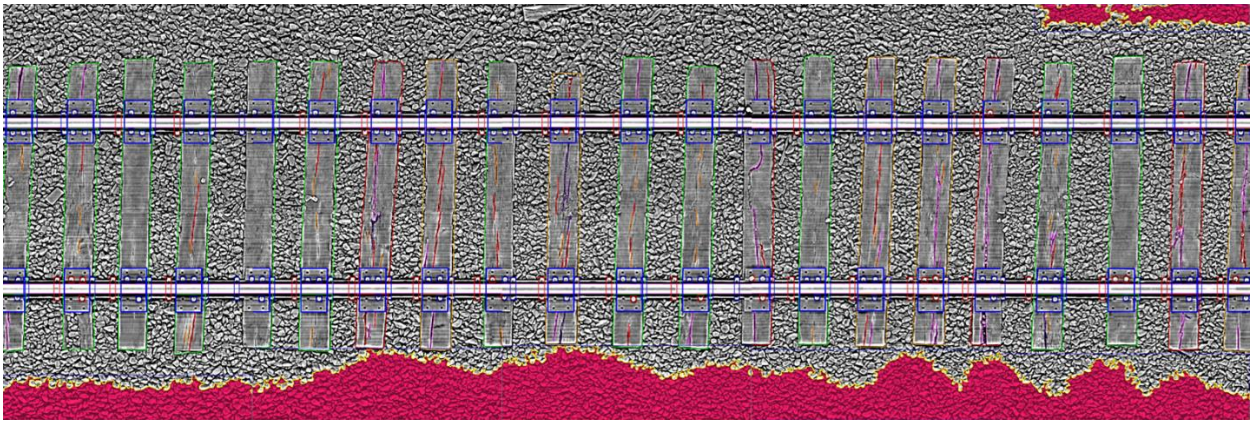

Figure 2.15: Example window for defective anchors

The correlation matrix (Table 2.10) shows a -0.13 correlation between the number of anchors and maximum gauge. This would indicate that the more anchors that are present in a window, the tighter the gauge is. However, this correlation is too weak to be visually observed in the scatter plot (Figure 2.16).

Table 2.10: Correlation matrix for spikes data

Geometry Parameter	Number of Defective Anchor	Number of Anchors	Max Distance to tie	Normalized Defective Anchors (%)
Max Gauge	0.00	-0.13	-0.05	-0.01
Min Left Profile 62	-0.02	0.08	0.01	-0.03
Max Left Profile 62	0.02	-0.07	-0.01	0.03
Min Right Profile 62	-0.02	0.08	0.01	-0.03
Max Right Profile 62	0.01	-0.08	-0.02	0.02
Min Left Profile Space Curve	-0.02	0.02	-0.01	-0.02
Max Left Profile Space Curve	0.00	-0.03	0.00	0.01
Min Right Profile Space Curve	-0.02	0.03	0.00	-0.02
Max Right Profile Space Curve	0.00	-0.04	-0.01	0.01
Min Left Alignment 62	0.00	0.01	-0.01	-0.01
Max Left Alignment 62	0.00	-0.02	0.01	0.01
Min Right Alignment 62	0.00	0.02	-0.01	-0.01
Max Right Alignment 62	0.00	-0.02	0.00	0.00
Min Left Alignment Space Curve	0.00	0.01	0.02	0.00
Max Left Alignment Space Curve	0.00	0.00	0.01	0.00
Min Right Alignment Space Curve	0.00	0.01	0.02	0.00
Max Right Alignment Space Curve	0.00	0.00	0.01	0.00
Max TQI	0.06	-0.05	0.02	0.06
Max Std. Mean Alignment	0.03	0.06	0.06	0.03
Max Std. Left Profile 62	0.05	-0.05	0.01	0.05
Max Std. Right Profile 62	0.05	-0.06	0.01	0.05
Max Std. Left Alignment 62	0.03	0.05	0.06	0.03
Max Std. Right Alignment 62	0.03	0.05	0.06	0.03
Average Cross Level	0.00	0.00	-0.01	-0.01
Average Curvature	0.01	0.02	0.00	0.00
Max Twist 31	0.01	-0.09	-0.02	0.01
Max Warp 62	0.01	-0.09	-0.02	0.01
Normalized Gauge	0.00	-0.13	-0.05	-0.01

The two regions of concentrated data in Figure 2.16 located around 72 and 40 anchors are due to the typical anchoring patterns of all crossties and every other crosstie anchored.

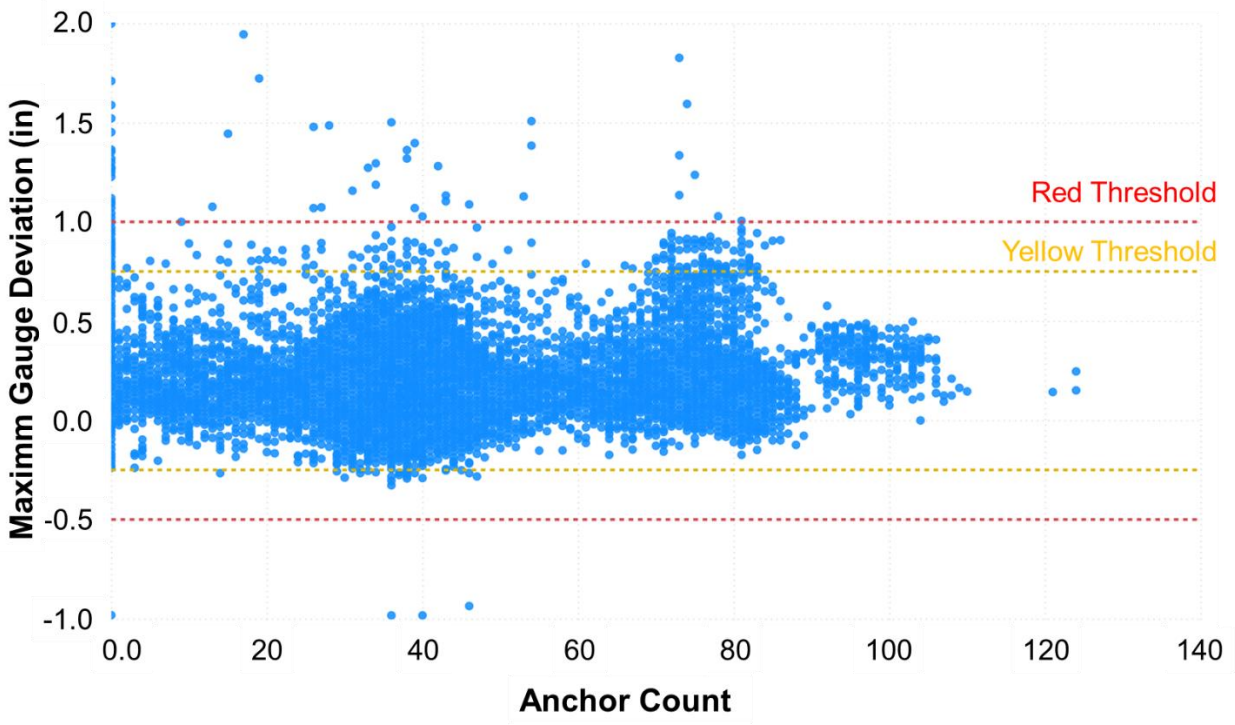

Figure 2.16: Scatter plot between maximum gauge deviation and anchor count

2.14 Ballast Surface Fouling

Fouled ballast is usually related to mud spots or other contaminated regions that include the intrusion of fine particles into the ballast later. From a track geometry perspective it mostly influences vertical parameters, namely surface (Goodarzi et al., 2020). The primary substructure inspection technology used in the rail industry is Ground Penetrating Radar (GPR). While GPR can output the layers of track substructure and identify the boundary between ballast and sub-ballast, LR*AI*L is capable of detecting superficial ballast fouling by comparing the grain sizes with normal ballast. If ballast particles are too small, the system outputs the area as fouled. The metric used for tracking areas of surface fouled ballast is the sum of fouled area per window.

The first example window (Figure 2.18) is located on a tangent with timber crossties. It has a mud spot with a total fouled area of 20.8 ft^2 (1.93 m^2). There is a yellow tag alignment defect and, although the profile does not show a defect, it varies considerably within the window (Figure 2.18).

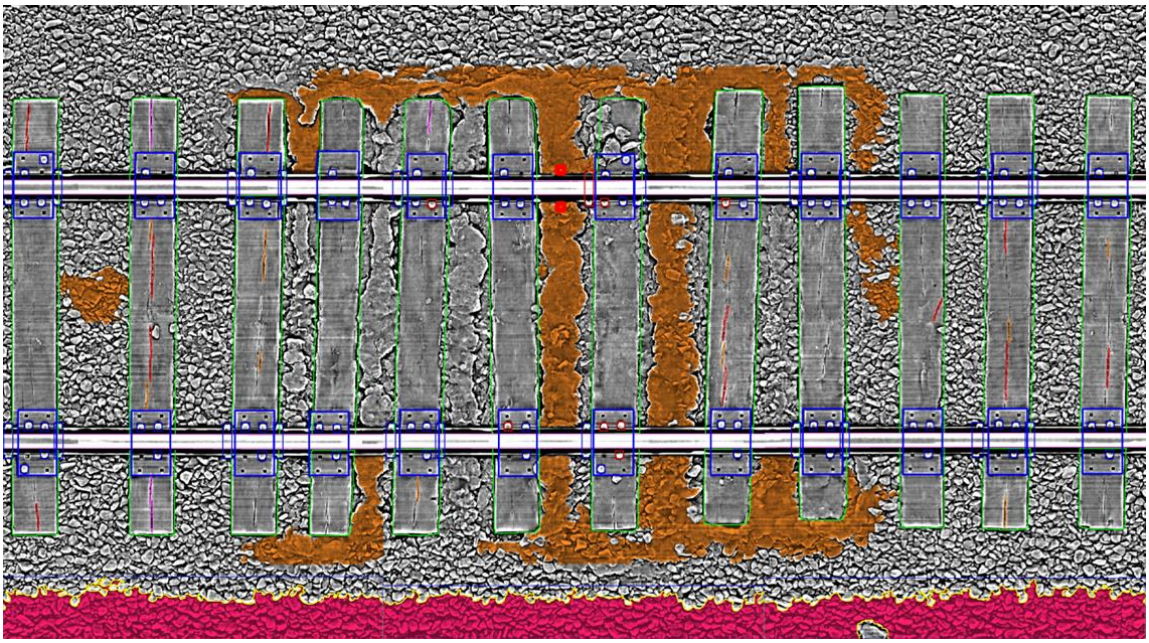

Figure 2.17: Example window for ballast surface fouling

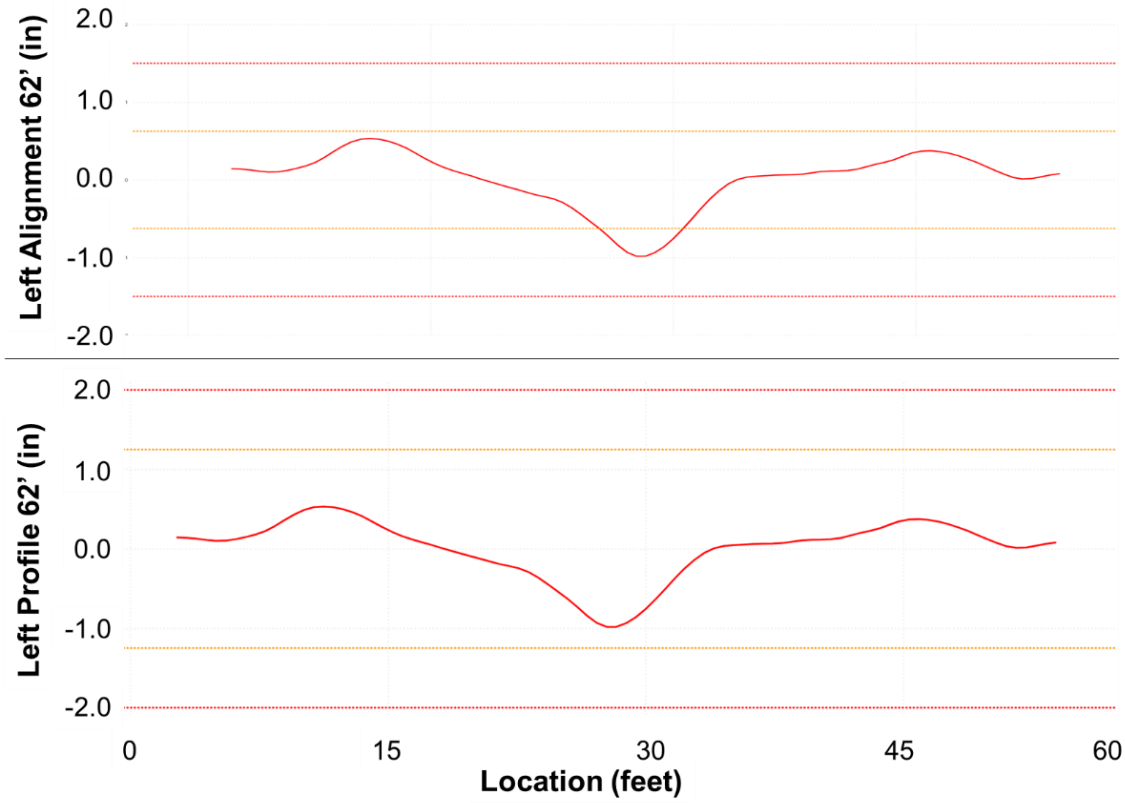

Figure 2.18: Alignment and profile strip chart for section with superficial ballast fouling

Although a few examples can be identified, when considering all the windows with superficial ballast fouling, there is no clear relationship between both variables when reviewing the scatter plot (Figure 2.19) and correlation matrix (Table 2.11). The highest correlation index found was 0.11 with maximum gauge and maximum TQI (as defined in Equation 2.1).

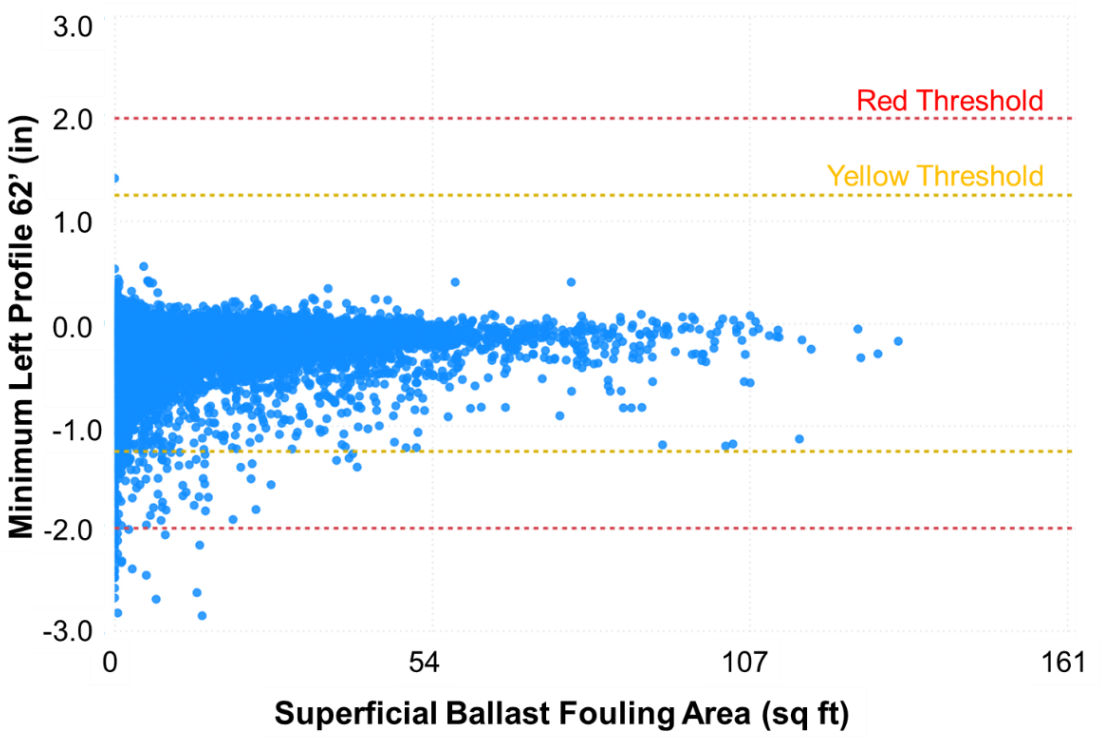

Figure 2.19: Scatter plot between minimum left profile and superficial ballast fouling area

Table 2.11: Correlation matrix for superficial ballast fouling

Geometry Parameter	Ballast Superficial Fouling
Max Gauge	0.11
Min Left Profile 62	-0.05
Max Left Profile 62	0.05
Min Right Profile 62	-0.04
Max Right Profile 62	0.05
Min Left Profile Space Curve	-0.03
Max Left Profile Space Curve	0.00
Min Right Profile Space Curve	-0.03
Max Right Profile Space Curve	0.00
Min Left Alignment 62	-0.02
Max Left Alignment 62	0.02
Min Right Alignment 62	-0.02
Max Right Alignment 62	0.02
Min Left Alignment Space Curve	0.01
Max Left Alignment Space Curve	-0.01
Min Right Alignment Space Curve	0.01
Max Right Alignment Space Curve	-0.01
Max TQI	0.11
Max Std. Mean Alignment	0.05
Max Std. Left Profile 62	0.11
Max Std. Right Profile 62	0.10
Max Std. Left Alignment 62	0.05
Max Std. Right Alignment 62	0.05
Average Cross Level	-0.01
Average Curvature	0.05
Max Twist 31	0.06
Max Warp 62	0.07
Normalized Gauge	0.11

2.15 Conclusion

A comparison of geometry and component datasets for the study corridor revealed no clear relationship between the two inspections. Although some examples can be found where both data types show irregularities, this is not strong enough to provide a correlation when

considering the whole subdivision, especially when including sections with and without irregularities. Even when comparing windows that all contain geometry deviations, no relationship was found with component inspection data.

This lack of relationship is likely due to two reasons. First, a single 115-mile (185 km) subdivision is not statistically relevant to draw this type of relationship due to the lack of diversity of track components and maintenance scrutiny. For example, a single subdivision is likely to have similar characteristics throughout, and it is difficult to find sections with different characteristics (e.g. track classes, tonnage, speed limits, grade, curvature), which makes the dataset more homogeneous and, thus, less statistically relevant. Second, this subdivision is very well maintained, which reduces the number of defective geometry and or components, creating some unbalance in the datasets. A statistically relevant dataset may require a network-level sampling of geometry and component data to better capture variability in track characteristics, components, maintenance procedures, and train operations.

However, when two different datasets are correlated with each other, this usually means that one of them is not needed and can be considered redundant. In this particular research problem, the lack or relationship between geometry and component inspection would indicate that both inspections should be carried out to best assess track component condition, efficiently and effectively plan maintenance activities, and ensure the safe movement of goods and people.

CHAPTER 3: TRACK DATA TRENDING

3.1 Introduction

As introduced and discussed in Chapter 1, railroads collect condition-related data on a variety of track components. Measurements can be captured at either a fixed distance or at an interval based on a specific asset (e.g., every crosstie or turnout). Measurements collected at a consistent interval (i.e. distance) along the track (e.g. rail wear and geometry) can be treated as a time series (Palese et al 2020) and visualized as a three dimensional (3D) graph (Figure 3.1).

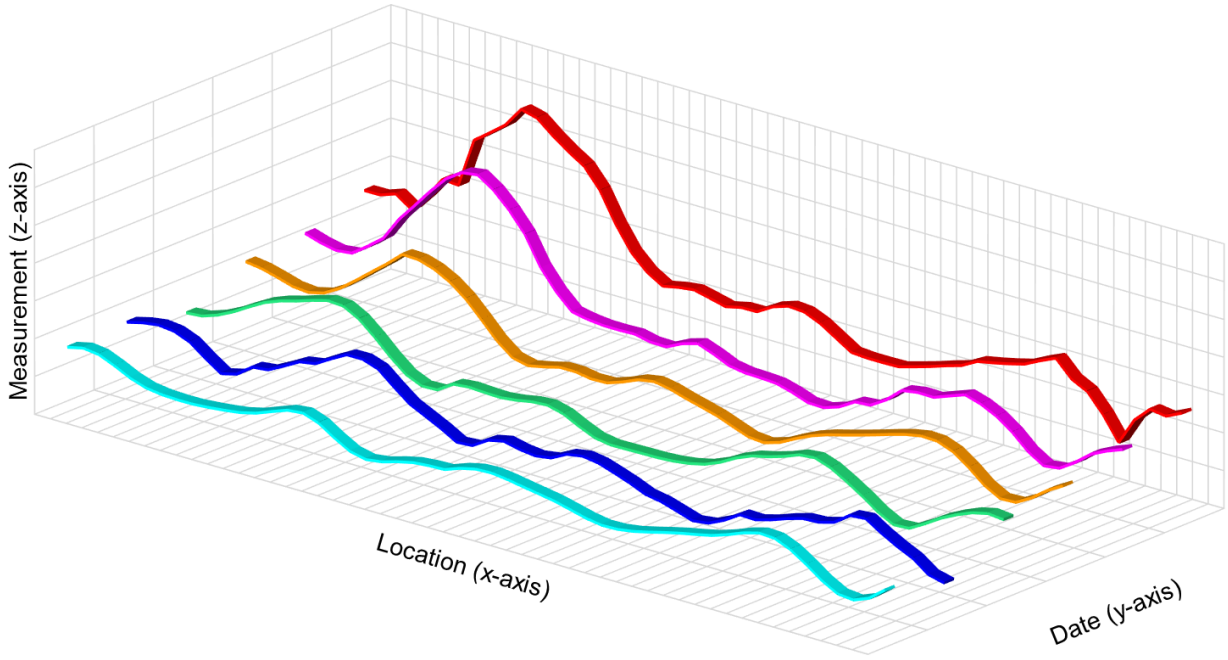

Figure 3.1: Conceptual three-dimensional qualitative graph of track geometry data

The x-axis represents the location along the track, referenced by milepost, track stationing, or some other linear metric. The y-axis represents the time domain, indicating when the measurement was taken, which can also be mapped to total accumulated tonnage or number of

axle passes, the latter of which is more common in transit applications. The z-axis presents the data collected for a given type of measurement (e.g., rail wear, gauge, etc.).

By breaking the 3D-graph (Figure 3.1) into two dimensions (2D), considering both the location and measurement axes, the data can be represented in a strip chart (Figure 3.2). Strip charts are commonly used in the railroad industry for visualization of track-related data and were introduced in Section 1.2.2.8. Each line on the graph represents a different data collection date.

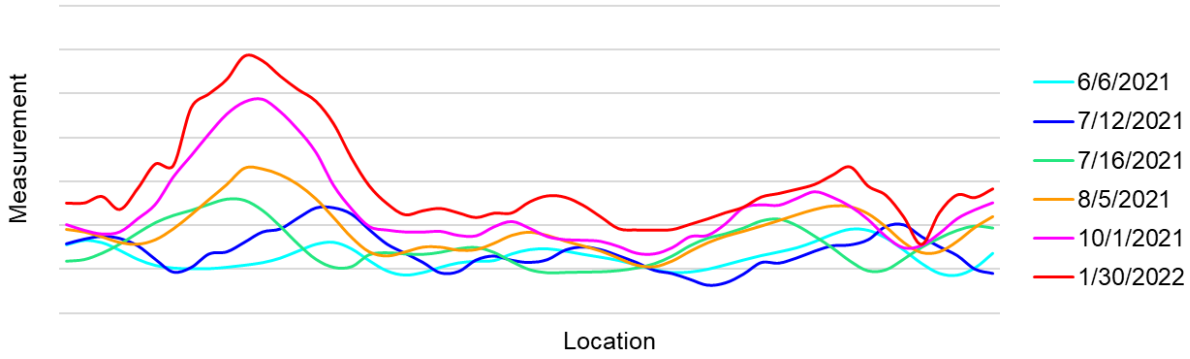

Figure 3.2: Example two-dimensional qualitative graph of track geometry data

Returning to the 3D graphic shown in Figure 3.1 and using the date (y-axis) and measurement (z-axis) axes, it is possible to visualize changes over time (Figure 3.3).

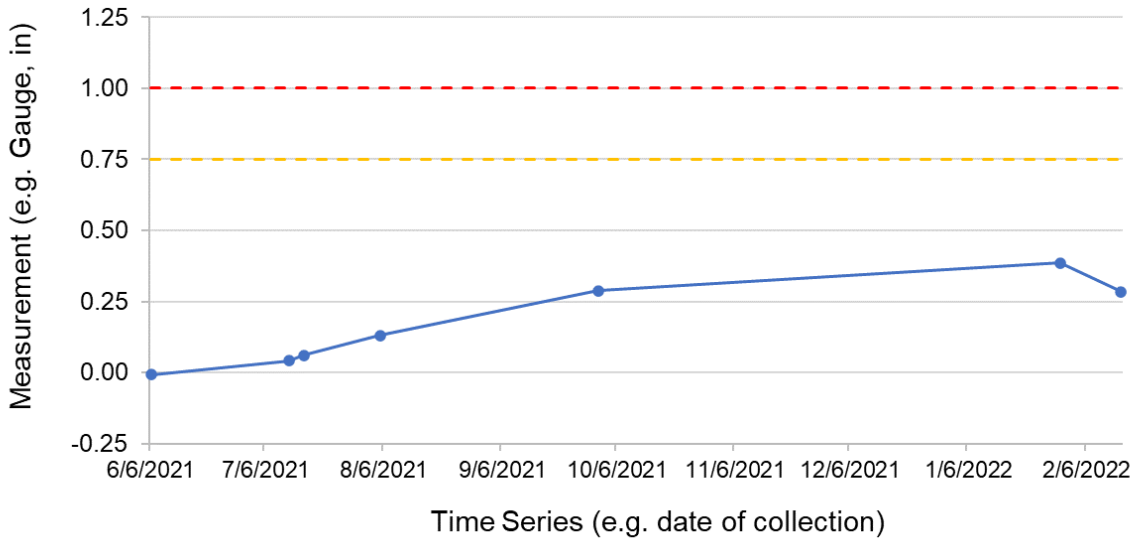

Figure 3.3: Two-dimensional graph of geometry data over time

Reducing the data points to a single value for each measurement requires a two-step process. First, the data must be windowed as discussed in Section 2.6. Second, a method for data aggregation within the window must be applied to generate a single value for each window (initially presented in Section 2.7). These steps are critical to data processing and reduce the amount of data that is presented to the end user. This type of data aggregation is consistent with upward movement in the pyramid (Section 1.4 and Figure 1.14).

3.2 Track Age and Accumulated Tonnage

The age of the track infrastructure and its components (represented on the x-axis) used in trending (modelling) refers to the life of the component (time since installation) or the time that has elapsed since the previous maintenance intervention. Geometry has been shown to deteriorate linearly with tonnage and is quantified in units of MGT (Million Gross Tons) per year (Caetano and Teixeira, 2016) or time (Esveld, 2014). For routes that have uniform traffic throughout the year (e.g. iron ore or coal-dominated routes) there is little difference between the

units of years or MGT. For transit systems, which use comparatively lightweight rolling stock, the age of track and its components can be tracked by means of number of axle passes (Iwnicki et al., 2000). The specific metric used will influence the deterioration rate output units given the unit will be determined by the age. For example, if the standard deviation of track geometry profile and MGT are used, the degradation rate will be output in units of inches/MGT or mm/MGT.

3.3 Track Degradation Model

Generation of a railroad track degradation model can identify a maintenance activity (e.g. tamping) can be divided into three phases (Figure 3.4): 1) the rapid deterioration of track geometry quality due to initial ballast settlement immediately after tamping, usually between 0.5 and 2 MGT (Lichtberger, 2005), 2) after the track is sufficient stabilized and starts to degrade linearly over the majority of the track's life and 3) the increasingly rapid deterioration, which can be exponential, and should be avoided since it can pose risks to safety, due to the rapid decrease in track quality (Guler et al., 2011; Esveld, 2014; Offenbacher et al., 2023).

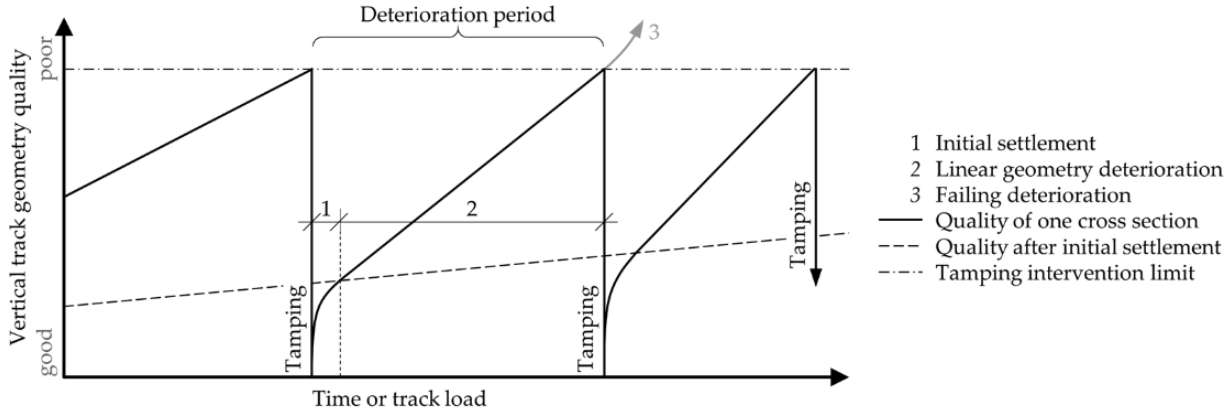

Figure 3.4: Theoretical track deterioration behavior over time (Offenbacher et al., 2023)

Different models can be used to compare the degradation of track condition over time and tonnage. Among the models that use only traditional computing and not machine learning, three models were selected for further evaluation in this research:

- Linear:

$$Y(t) = a * t + b \quad \text{Eq. 3.1}$$

- Logarithmic:

$$Y(t) = a * \ln(t) + b \quad \text{Eq. 3.2}$$

- Exponential:

$$Y(t) = e^{a*t} * b \quad \text{Eq. 3.3}$$

Where *Y(t)* is the parameter at a certain time, *t* is time, and *a* and *b* are regression parameters. The variable *a* is commonly used to describe the degradation rate and *b* is related to the initial value of the parameter. I will evaluate the effectiveness of the three models by comparing the median values of the coefficient of determination (R^2) error function to assess the most suitable regression model for each data aggregation function.

3.4 Methodology

To evaluate the suitability of the proposed trending frameworks for geometry and component data, three different regression models (Section 3.3) will be applied to the aggregated data (Section 2.7) within each of the chosen windows (Section 2.6). The results of each model will be compared using R^2 coefficients. To compare all windows within the sample data the median R^2 will be used. Localized maintenance information was not available thus there was no means to easily identify locations that had unique maintenance and degradation cycles.

3.5 Results

3.5.1 Geometry Data Trending

Results of the regression models for track geometry are presented in Table 3.1, rank ordered by linear median R^2.

Table 3.1: Regression Results for Geometry Data

Parameter	Median R^2		
	Linear	**Log**	**Exp**
Max TQI	0.126	0.058	0.123
Max Gauge	0.119	0.082	0.115
Min Left Profile Space Curve	0.086	0.049	0.071
Max Left Profile Space Curve	0.086	0.049	0.074
Min Right Profile Space Curve	0.082	0.046	0.069
Min Left Alignment 62	0.080	0.050	0.063
Max Left Alignment 62	0.080	0.050	0.075
Min Right Alignment 62	0.079	0.049	0.061
Max Std. Left Profile 62	0.079	0.050	0.075
Max Right Profile 62	0.077	0.047	0.072
Max Right Profile Space Curve	0.074	0.042	0.064
Max Std. Right Profile 62	0.071	0.043	0.068
Overall	**0.049**	**0.033**	**0.042**
Max Left Alignment Space Curve	0.045	0.036	0.035
Min Left Alignment Space Curve	0.044	0.035	0.029
Min Right Alignment Space Curve	0.044	0.035	0.029
Max Right Alignment Space Curve	0.043	0.036	0.034
Max Left Alignment 62	0.043	0.029	0.038
Min Left Alignment 62	0.043	0.029	0.030
Min Right Alignment 62	0.041	0.028	0.028
Max Right Alignment 62	0.039	0.028	0.034
Max Twist 31	0.035	0.018	0.030
Max Warp 62	0.034	0.015	0.030
Average Curvature	0.021	0.012	0.019
Max Std. Left Alignment 62	0.016	0.015	0.014
Max Std. Right Alignment 62	0.015	0.010	0.013
Average Crosslevel	0.011	0.029	0.018

The majority of the median R^2 values are very low, and well below the value of 0.5 that is commonly used as a threshold between a reasonable or poor fit. Additional details on the R^2 error function are provided in Section 3.6.2.

The low median R^2 values may be influenced by outliers which include measurement errors in frogs and grade crossings and the occurrence of flat lines, when the system is not capable of producing good measurements (e.g. low speed operation). The measurements in windows with this issue (Figure 3.5) are noisy and those windows can be detected by a very low R^2 value.

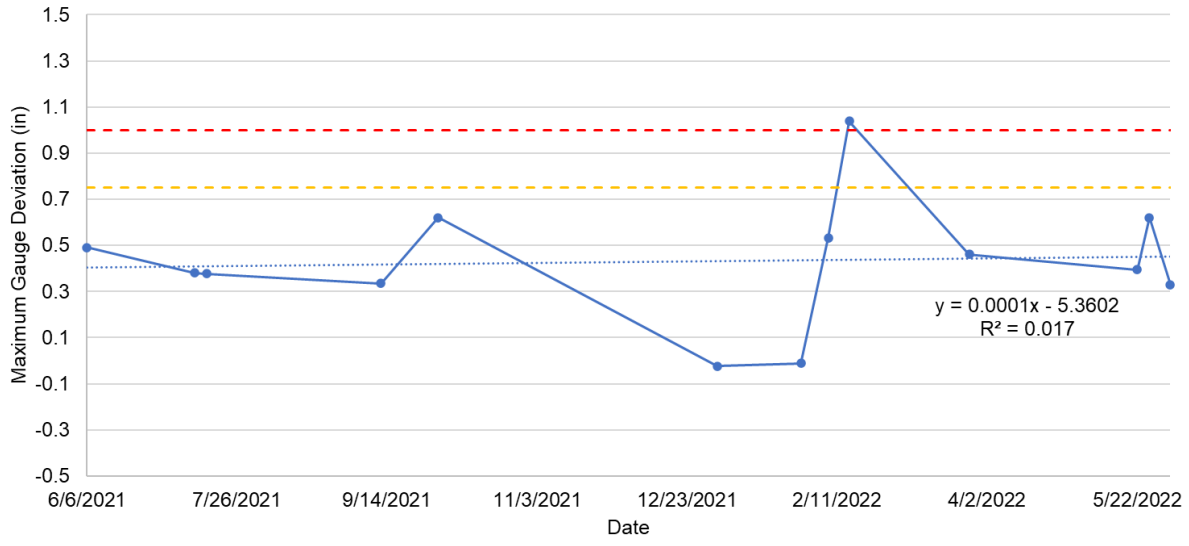

Figure 3.5: Example track window with outliers

Since geometry data were collected using an ATGMS, data cleaning is undertaken off of the vehicle in post processing within an asset management platform. In a revenue service application with high frequency data collection (e.g. three times a week) outliers do not pose an challenge given the error would be diluted over multiple measurements. However, in this project which consumes approximately one inspection run of data per month, outliers may decrease the R^2 coefficient appreciably.

Track maintenance activities are expected to increase the quality of track, thereby generating significant changes to the parameters within that window (Goodarzi et al., 2020; Offenbacher et al., 2023). When analyzing a single window, this change is noted by a significant drop in the data (Figure 3.6). When maintenance is conducted, a new degradation cycle begins for that window and trending should be reset. If the trend is not reset (e.g. considering all the maintenance cycles without separation) this may lead to a negative slope and a low R^2 value, usually below 0.5. Resetting the trend can increase the R^2 for both maintenance cycles. Goodarzi et al. (2020) and Neuhold et al. (2020) have developed automated methods to detect maintenance based on the principles described here. Since maintenance records were not provided from the partner railroad the maintenance cycle separation was not undertaken and this may have influenced the low R^2 values.

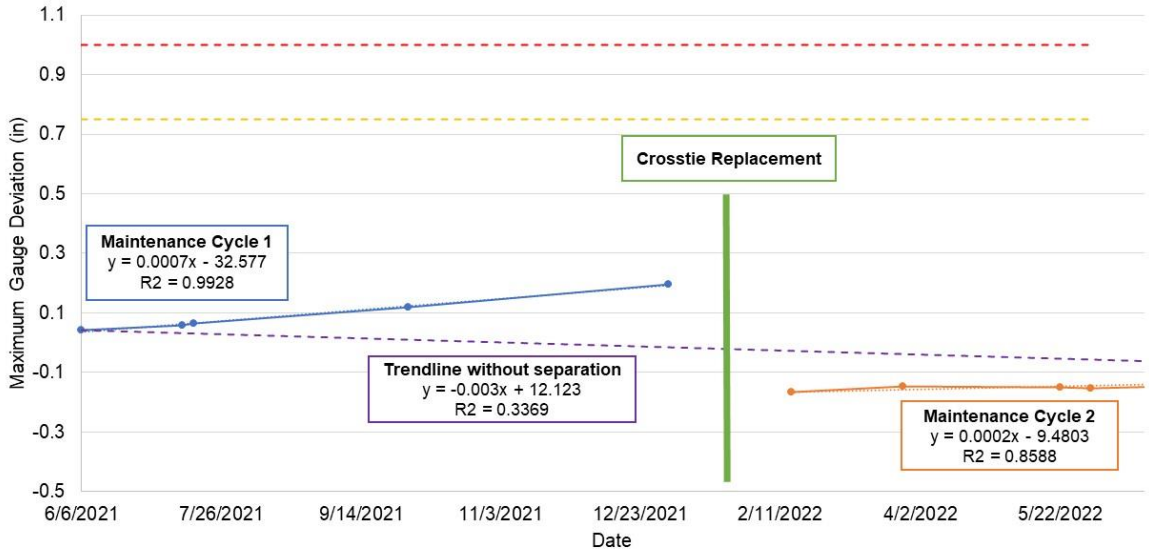

Figure 3.6: Example track window with maintenance activity

In the context of this project R^2 values measure how well the variance in one parameter (e.g. gauge) is explained by the other parameter (e.g. time). This means, for example, that if the

gauge is not varying with time or tonnage the R^2 will be very low (Figure 3.7). This is a common occurrence when the tracks are well maintained and/or have very low degradation rates (e.g. a low slope). While this does not present an issue in practice and only indicates that no maintenance is required in that section, it is likely to be reflected in low median R^2 values.

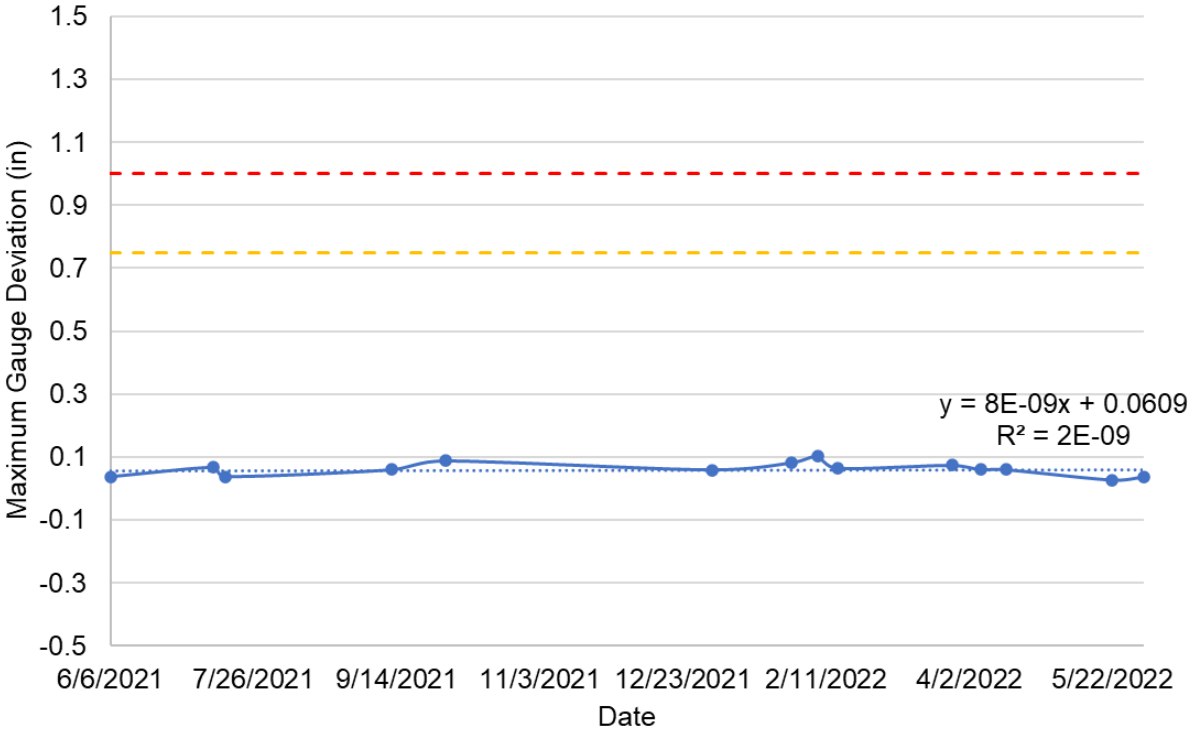

Figure 3.7: Example track window with low slope and correspondingly low R^2 value

TQI and maximum gauge are the parameters with the highest R^2 values. With the exception of the average of crosslevel, the linear regression model provides better median R^2 values than an exponential or logarithmic function.

As identified by Esveld (2014), the linear degradation phase encompasses the majority of the life of the tracks, hence its higher R^2 values. The initial logarithmic and final exponential phases are difficult to model and are not the focus of this research. These rates are important for modeling and tracking of initial degradation of ballast after tamping and other end-of-life

questions related to crossties and fastening systems. The scope of this work is developing and validating a model to detect rate of change over the majority of the life of the track.

For most of the aggregation functions the R^2 value for both linear and exponential models were very close. This is largely due to the fact that the parameters chosen for the exponential model were relatively small and it thereby demonstrated minimal curvilinear behavior.

3.5.2 Component Data Trending

The results of the component trending regression models are presented in Table 3.2.

Table 3.2: Regression Results for Component Data

Component	Parameter	Median R^2		
		Linear	Log	Exp
Fouling	Ballast Superficial Fouling	0.392	0.212	0.212
Crosstie	Average Crosstie Rating	0.299	0.184	0.299
Crosstie	Weighted Crosstie Rating	0.299	0.185	0.298
Crosstie	Normalized Defective Crossties	0.276	0.177	0.136
Crosstie	Number of Defective Crossties	0.276	0.181	0.142
Tie Plate	Normalized Defective Tie Plates	0.276	0.138	0.194
Fastener	Number of Defective Fasteners	0.274	0.210	0.109
Tie Plate	Number of Defective Tie Plates	0.274	0.137	0.193
Anchor	Number of Defective Anchors	0.274	0.122	0.240
Anchor	Normalized Defective Anchors	0.274	0.124	0.240
Fastener	Normalized Defective Fasteners	0.274	0.196	0.109
	Overall	**0.274**	**0.162**	**0.197**
Anchor	Number of Anchors	0.240	0.191	0.197
Anchor	Max Distance to Tie	0.209	0.192	0.156
Spike	Normalized Defective Spikes	0.166	0.139	0.118
Spike	Number of Defective Spikes	0.156	0.136	0.113

Component data demonstrate similar behavior as geometry data, with both linear and exponential results lying very close to one another. The aggregation functions that best explain crosstie degradation are average crosstie rating and weighted crosstie rating.

For other components, there is little difference between the absolute number of defective components in the window and the normalized number of defective components per window. This can be explained by the low variation in the number of components in each window since crosstie spacing is largely consistent throughout the test corridor.

In summary, linear regression yields the highest median R^2 values from among the three regression models, thus it was selected for use in this research.

3.6 Discussion

Compared to exponential and logarithmic regressions, the linear model has notable advantages. Linear models are easy to interpret (Liao et al., 2022) given they are described by simple variables, thereby providing information to many levels of the railroad organizational structure. Vulnerabilities of a linear track degradation model occur during early and late portions of the track life cycle. These should be given due attention depending on the model's objectives, but for most of the life cycle of track, its degradation is linear (Esveld, 2014).

A linear model is most notably described by the slope (related to the degradation rate) and the intercept (related to the initial quality of maintenance) (Esveld, 2014). Other parameters used in this research are the error function and last value obtained. The error function is used to assess the goodness of the linear fit and identify outliers. The last value obtained is relevant for data trending and indicates whether the segment is close to the specified defect threshold (Neuhold et al., 2020) (Figure 3.8). These elements of linear trending will be described in more detail in the next sections.

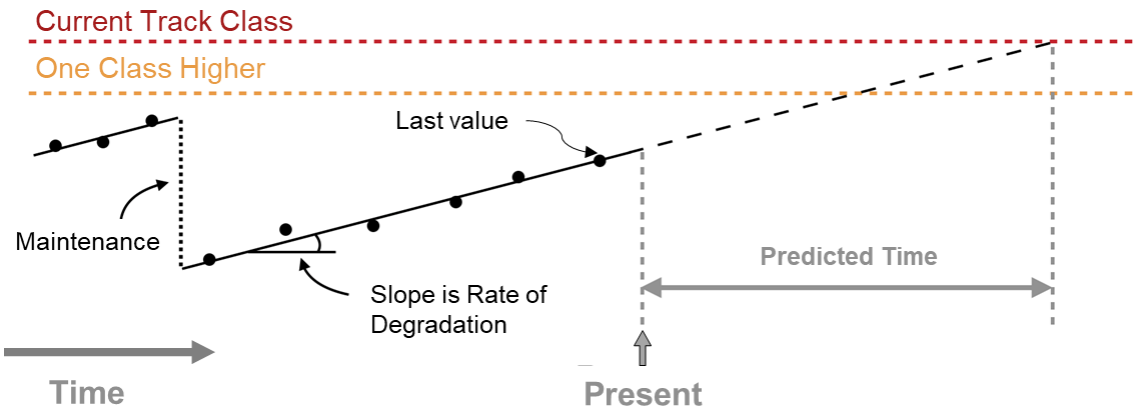

Figure 3.8: Elements of the linear trending and track degredation prediction

3.6.1 Slope

The slope of the linearly-fitted line indicates the rate (or speed) at which the parameter is degrading. It has the units of the *measured parameter* divided by the *age* referenced from the time since installation or the previous maintenance intervention. In the example case of gauge and tonnage (MGT), the units are inches/MGT or mm/MGT. A section with a higher slope will reach the pre-established geometry thresholds faster than a window with smaller slope. Figure 3.9 provides two example track sections with linear slopes calculated for maximum gauge over a window of 30 feet (9.14 m). Section 1 (orange line) has a higher slope (0.0008 inches/day or 0.292 inches/year) whereas Section 2 (blue line) has a lower slope (0.0003 inches/day or 0.109 inches/year). Section 1 (orange) will require maintenance sooner than Section 2 (blue).

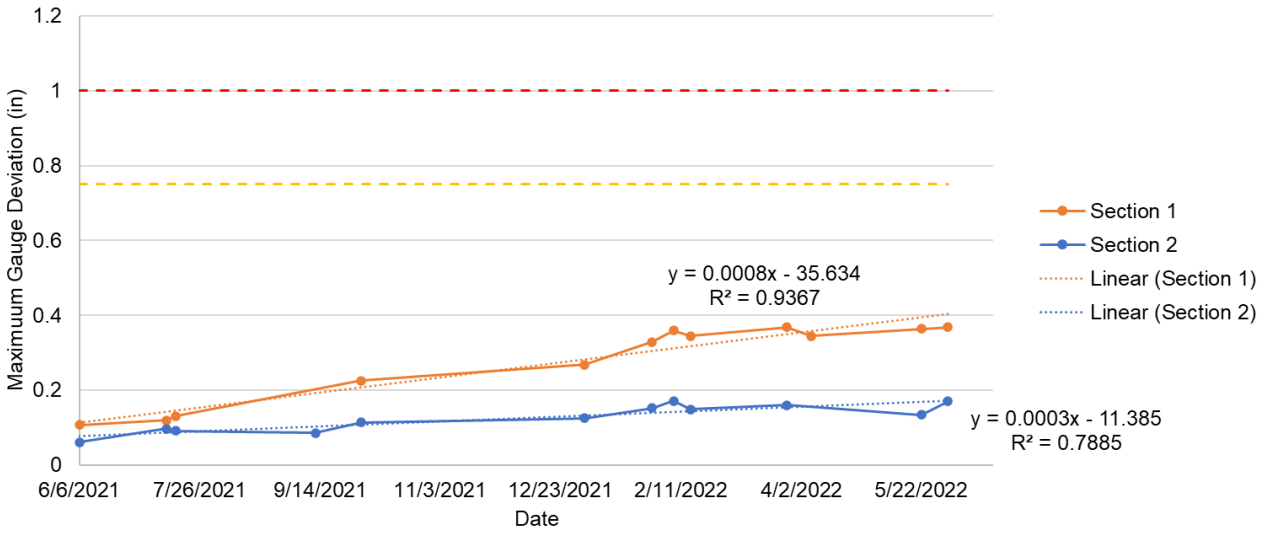

Figure 3.9: Example data from track windows with high and low degredation slopes

3.6.2 Error Function

The error function is used to estimate the goodness of fit of the linear regression model for a set of data. The error of a linear model is commonly quantified using the coefficient of determination (R^2) (Neuhold et al. , 2020) using Equation 3.4:

$$R^2 = \frac{\sum_{i=1}^{n}(\hat{y}_i - \bar{y})^2}{\sum_{i=1}^{n}(y_i - \bar{y})^2} \qquad \text{Eq. 3.4}$$

where $\hat{y}_i$ is a point on the regression line, $\bar{y}$ is the mean value of all measurements and y_i is measured point.

The R^2 value describes the proportion of variance within the data that is explained by the model. If the model perfectly describes the data the value for R^2 is one. If the model fails to describe any of the variance in the data, its R^2 would be zero. However, if the model has small variance (e.g. a flat line, no variation over time) the R^2 is also at or near zero, even though there is likely a good fit. This does not present a challenge for track maintenance applications since the railroads are interested in the windows which have higher variation over time (not flat lines

indicative of track that is showing little or no change). Even including flat line cases the R^2 value is suitable for evaluating the model's suitability. R^2 values can also be used to detect outliers that may be measurement errors. If left untreated, these can cause the model to output incorrect results.

In any case, R^2 is a proven and trustworthy metric that can be used for filtering the relevant windows for practical planning of maintenance and evaluation of track degradation rates. Depending on the application and data collection methods used, a reasonable R^2 threshold of 0.5 must be met for the trend to be considered valid.

3.6.3 Last Value

If the aggregation function (defined in Chapter 2) is related to the regulatory thresholds (defined in Chapter 1) then the last measured value will indicate how close to the threshold the track geometry parameter is for a given window. Figure 3.10 presents an example of left profile that shows a negative trend where the last value already exceeds the yellow threshold and is getting close to the red threshold. The red threshold is commonly used by the railroads to denote the posted (actual) class threshold per the FRA (2022) CFR 213 regulations. The yellow threshold is usually one class higher (i.e. more strict than the actual class) and is used for preventative maintenance purposes. Unlike the red threshold, exceedance of the yellow threshold does not necessitate a speed restriction. In this example window (Figure 3.10) there is already a yellow tag defect given the last value of -1.8 in (45.7 mm) exceeds the threshold of 1.25 in (32 mm).

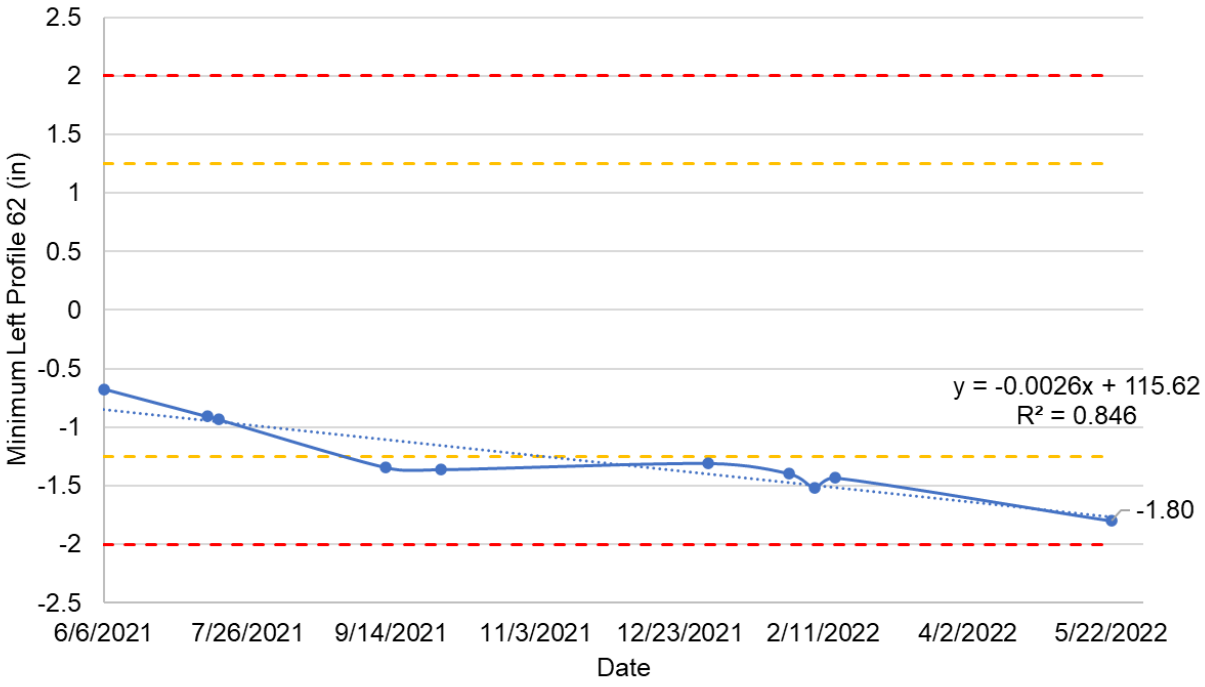

Figure 3.10: Left profile (62 ft chord) trending close to the red threshold

3.6.4 Initial Quality

The intercept (*b* parameter in the linear equation) represents the initial quality of the track or the state of the track after a maintenance intervention (Esveld, 2014). When comparing consecutive maintenance cycles, the initial quality is the quality achieved immediately after the maintenance activity and is the highest quality that that particular section will experience during the maintenance cycle. The initial condition of a track segment has a notable influence on the life cycle of the tracks, thus a small decrease in initial quality can shorten the maintenance cycle by a few months or tens of MGTs (Tzanakakis, 2013).

The difference between the last measurement of the previous maintenance cycle and the first measurement of the next cycle can be used as a proxy metric for the effectiveness of maintenance. This value is especially useful for tamping activities where the profile standard deviation can be used (Offenbacher et al., 2023). This is particularly helpful when using high

frequency (e.g. three times a week) geometry measurements provided by ATGMS since it is possible to capture the initial quality of the tracks prior to degradation, right after the maintenance activity (Bilheri et al., 2023). If the start of a new degradation cycle (after maintenance is conducted) is not known, the initial value should not be used for assessing maintenance quality given it is likely to overestimate the initial quality (and underestimate degradation rate) due to the scarcity of early life cycle data.

3.7 Conclusions

Comparing linear regression with logarithmic and exponential models has shown that linear regression is suitable for modeling the majority of a track segment's life cycle. In addition to its utility in interpreting track geometry data a linear model is also suitable for assessing track component degradation data. The primary advantage of a linear model is its simplicity and ability to be easily interpreted by many levels within the railroad organizational structure. The variables used in the linear equation explain practical aspects of the track, including degradation rate, initial quality, and regulatory defects and compliance. These values can be used by railroads to build more effective and efficient maintenance plans.

CHAPTER 4: CONCLUSIONS AND FUTURE WORK

This thesis explores the domain of railroad track geometry and component health data by presenting common data types, describing how the railroads commonly use these data, and introducing a framework that can be used to trend datasets and draw actionable conclusions about track and component life cycle.

Chapter 1 describes the current federal regulatory requirements for track inspection in the US, summarizes the types of components and data, and provides an overview of track geometry inspection equipment and their advantages and disadvantages. It also proposes a theoretical corporate track inspection data use and aggregation pyramid for a railroad. In Chapter 2 the relationship between track geometry and component data is explored, and I present windowing and aggregation concepts. Lastly, Chapter 3 presents a framework for data trending and compares three regression models through the application of revenue service Class I data.

4.1 Summary of Findings

4.1.1 Investigation into the Relationship Between Track Component Health and Track Geometry Data (Chapter 2)

Fixed 30 feet (9.14 m) windows and aggregation functions were used to compare track geometry and component data. Both datasets were collected using different vehicles on the same 115-mile (185 km) subdivision. The data were aligned using fixed assets that were provided by the host railroad. Correlation matrices and scatter plots showed no correlations between the two datasets. This suggests that railroads should consider the use of both technologies to comply with federal regulations, maintain a good state-of-repair, and ensure the safe movement of trains.

4.1.2 Track Data Trending (Chapter 3)

Using the same fixed window and aggregation functions described in Chapter 2, a trending framework was developed. Linear, logarithmic, and exponential regression models were tested. The linear model generated the best results for both datasets using R^2 values. Although the median R^2 values were consistently low among all models, the linear model has utility for maintenance planning as elements of it are specifically useful in explaining track degradation. The slope of the linear model represents the degradation rate in a particular window, the last measured value indicates whether the window is close to an FRA (or other) defect threshold, and the error function (R^2) can be used to detect outliers or windows that do not need maintenance.

4.2 Recommendations and Future Work

The collection and use of track-related data has evolved from a find-and-fix system primarily designed to comply with regulatory requirements to incorporate big data and data science, especially when using ATGMS. The increasing volume of data generated by inspection systems has required railroads to develop innovative strategies to ingest, store, and process data. Through processing and refining these datasets, information is generated to achieve higher levels of the data pyramid (Chapter 1) which presents less (but more aggregated) data to railroad decision makers.

Beyond traditional (laser-based) collection of track geometry data, technologies such as image vision, combined with AI models, can objectively characterize important track-related health information including crosstie, fastening system, and ballast condition. However, the relationship between these two datasets has not shown promising results to date. This is likely

due to the data used in this research only considering one subdivision, with little variability in track components, design, and use. Applying the same framework presented here to a broader dataset with multiple subdivisions, track designs, annual traffic, and train operating speeds could increase the correlation between geometry and component data. Another possibility for future work is to investigate the relationship between geometry and component inspection data as a function of time / tonnage (e.g. study the trending of both gauge and crosstie rating at the same track window).

Specifically, when comparing geometry and component data, data alignment plays a very important role. However, there are significant data alignment challenges when using disparate datasets collected with multiple technologies and platforms, on different dates, with different sample collection rates. One way to avoid this alignment challenge is having both geometry and component collection devices installed in the same vehicle, and this is the direction at least one Class I railroad is heading through the use of ATGMS.

However, both the geometry and component data analyzed in this study have small R^2 values. This does not pose a practical problem when the model is used by a railroad company but does cause a problem in model validation. To dilute the effect of outliers (e.g. measurement errors) data from high frequency (e.g. every three days) geometry collection can be used. Additionally, including a data cleaning step to remove spike and flat lines would increase the quality of the initial dataset and its resulting output. Using track maintenance information from the railroad or detected automatically from the dataset to reset the trending windows has the potential to increase the accuracy of the model and can help railroad objectively assess the quality of maintenance activities.

REFERENCES

Alsahli, A., A.M. Zarembski, J.W. Palese and T.L. Euston. 2019. Investigation of the Correlation Between Track Geometry Defect Occurrence and Wood Tie Condition. *Transportation Infrastructure Geotechnology*, 6: 226–244.

Andrews, J. 2013. A modelling approach to railway track asset management. *Proceedings of the Institution of Mechanical Engineers, Part F: Journal of Rail and Rapid Transit*, 227(1): 56–73.

Audley, M. and J. Andrews. 2013. The effects of tamping on railway track geometry degradation. *Proceedings of the Institution of Mechanical Engineers, Part F: Journal of Rail and Rapid Transit*, 227(4): 376–391.

Bilheri, A., A. Merheb and I. Aragona. 2023. Big data in railroads: the use of unmanned inspection vehicles. In: *Proceedings Of The 12th International Heavy Haul Association Conference 2023 (IHHA RIO 2023)*, Rio de Janeiro, Brazil.

BNSF Railroad. 2021. Geo Car Technologies Detect What The Eye Can't. URL https://www.bnsf.com/news-media/railtalk/innovation/geo-cars.html. Accessed 2023-10-20.

Caetano, L. and P. Teixeira. 2016. Predictive Maintenance Model for Ballast Tamping. *Journal of Transportation Engineering*, 142: 04016006.

Carr, G.A., A. Tajaddini and B. Nejikovsky. 2009. Autonomous Track Inspection Systems – Today and Tomorrow. In: *Proceedings Of The 2009 American Railway Engineering And Maintenance Of Way Association Annual Conference*, American Railway Engineering and Maintenance-of-Way Association, Chicago, IL, USA.

Daniel, W.W. 1990. *Applied Nonparametric Statistics*, 1st ed. PWS-KENT Pub., Boston, MA, USA.

Zwarthoed-van Nieuwenhuizen, D., (Ed.) . 2001. *Modern Railway Track (2001)*, 2nd ed. Delft University of Technology, Delft, Netherlands.

Esveld, C. 2014. *Modern Railway Track (2014)*, Digital ed. MRT-Productions, La Couronne, Nouvelle-Aquitaine, France.

Federal Railroad Administration (FRA). 2022. Part 213 - Track Safety Standards, In: *Title 49 of the Code of Federal Registrations*. US Department of Transportation, Federal Railroad Administration, Washington, DC, USA. pp.100–154.

Fendrich, L. & W. Fengler, (Eds.) . 2019. *Handbuch Eisenbahninfrastruktur*, 2nd ed. Springer, Berlin, Heidelberg.

Goodarzi, S., H.F. Kashani, J. Oke and C.L. Ho. 2020. Data-Driven Methods to Predict Track Degradation: A Case Study. *Construction and Building Materials*, (344): 17.

Guler, H., S. Jovanovic and G. Evren. 2011. Modelling railway track geometry deterioration. *Proceedings of the Institution of Civil Engineers - Transport*, 164(2): 65–75.

Harrington, R., J.R. Edwards, A. de O. Lima, M.S. Dersch, R. Fox-Ivey, J. Laurent and T. Nguyen. 2022. Use of Deep Convolutional Neural Networks (DCNNs) and Change Detection Technology for Railway Track Inspections. *Proceedings of the Institution of Mechanical Engineers, Part F: Journal of Rail and Rapid Transit*,: 1–9.

Hay, W.W. 1982. *Railroad Engineering*, Second ed. John Wiley & Sons, New York, NY, USA.

Iwnicki, S., S. Grassie and W. Kik. 2000. Track Settlement Prediction Using Computer Simulation Tools. *Vehicle System Dynamics*.

Jovanovic, S. 2004. Railway Track Quality Assessment and Related Decision Making. In: *2004 IEEE International Conference On Systems, Man And Cybernetics*, The Hague, Netherlands, pp. 5038–5043.

Keylin, A. 2019. *Measurement And Characterization Of Track Geometry Data: Literature Review And Recommendations For Processing FRA ATIP Program Data | FRA*. FRA.

Liao, Y., L. Han, H. Wang and H. Zhang. 2022. Prediction Models for Railway Track Geometry Degradation Using Machine Learning Methods: A Review. *Sensors*, 22(19): 7275.

Lichtberger, B. 2005. *Track Compendium. Formation, Permanent Way, Maintenance, Economics*, First Edition ed. Eurailpress, Hamburg.

Neuhold, J., I. Vidovic and S. Marschnig. 2020. Preparing Track Geometry Data for Automated Maintenance Planning. *Journal of Transportation Engineering, Part A: Systems*, 146(5): 04020032.

Offenbacher, S., C. Koczwara, M. Landgraf and S. Marschnig. 2023. A Methodology Linking Tamping Processes and Railway Track Behaviour. *Applied Sciences*, 13(4): 2137.

Offenbacher, S., J. Neuhold, P. Veit and M. Landgraf. 2020. Analyzing Major Track Quality Indices and Introducing a Universally Applicable TQI. *Applied Sciences*, 10(23): 8490 DOI: 10.3390/app10238490.

Palese, J.W., A.M. Zarembski and N. Attoh-Okine. 2020. Methods for Aligning Near-Continuous Railway Track Inspection Data. *Journal of Rail and Rapid Transit*, 234(7): 709–721.

Quiroga, L.M. and E. Schnieder. 2010. A heuristic approach to railway track maintenance scheduling. In: *Computers In Railways XII*, Beijing, China, pp. 687–699.

RailPod. 2021. RailPod, Inc. – Comprehensive Track Data for Safer Railroads. URL https://rail-pod.com/. Accessed 2023-10-20.

Railway Track and Structures. 2020. Norfolk Southern Debuts Autonomous Track Inspection Technology Mounted on Locomotive. URL https://www.rtands.com/railroad-news/norfolk-southern-debuts-autonomous-track-inspection-technology-mounted-on-locomotive/. Accessed 2023-10-20.

Roadcap, T., B. Kerchof, M.S. Dersch, M. Trizotto and J.R. Edwards. 2019. Field Experience and Academic Inquiry to Understand Mechanisms of Spike and Screw Failures in Railroad Fastening Systems. In: *Proceedings Of The 2019 AREMA Annual Conference With Railway Interchange*, AREMA, Minneapolis, MN, pp. 10.

Salvador, S. and P. Chan. 2007. Toward accurate dynamic time warping in linear time and space. *Intelligent Data Analysis*, 11(5): 561–580.

Scott, G., E. Chillingworth and M. Dick. 2010. Development of an Unattended Track Geometry Measurement System. American Society of Mechanical Engineers Digital Collection, pp. 383–387.

Sharma, S., Y. Cui, Q. He, R. Mohammadi and Z. Li. 2018. Data-Driven Optimization of Railway Maintenance for Track Geometry. *Transportation Research Part C: Emerging Technologies*, 90: 34–58.

Soufiane, K., A.M. Zarembski and J.W. Palese. 2022. Effect of Adjacent Support Condition on Premature Wood Crosstie Failure. *Transportation Infrastructure Geotechnology*, 9(3): 302–320.

Soufiane, K., A.M. Zarembski and J.W. Palese. 2023. Forecasting cross-tie condition based on the dynamic adjacent support using a theory-guided neural network model. *Proceedings of the Institution of Mechanical Engineers, Part F: Journal of Rail and Rapid Transit*,: 09544097231203275.

Sung, L. 2005. *Development Of Objective Track Quality Indices*. FRA, RR05-01.

Tzanakakis, K. 2013. *The Railway Track And Its Long Term Behaviour*, 1st ed. Springer Berlin, Heidelberg.

Xu, P., R. Liu, Q. Sun and L. Jiang. 2015. Dynamic-Time-Warping-Based Measurement Data Alignment Model for Condition-Based Railroad Track Maintenance. *IEEE Transactions on Intelligent Transportation Systems*, 16(2): 799–812.

Zarembski, A.M. 2014. Some examples of big data in railroad engineering. In: *2014 IEEE International Conference On Big Data (Big Data)*, pp. 96–102.

Zarembski, A.M., D. Einbinder and N. Attoh-Okine. 2016. Using multiple adaptive regression to address the impact of track geometry on development of rail defects. *Construction and Building Materials*, 127: 546–555.

Zarembski, A.M. and D.R. Holfeld. 1997. On the Prediction of the Life of Wood Crossties. , Pittsburgh, PA.

Zarembski, A.M., J.W. Palese and T.L. Euston. 2017. Correlating Ballast Volume Deficit with the Development of Track Geometry Exceptions Utilizing Data Science Algorithm. *Transportation Infrastructure Geotechnology*, 4: 37–51.